SANDIA REPORT
SAND2007-2319
Unlimited Release
Printed March 2008

Experiments for Calibration and Validation of Plasticity and Failure Material Modeling: 6061-T651 Aluminum

Sam X. McFadden
Ken L. Lee
John S. Korellis
Brendan R. Rogillo
Paul W. Hatch

Prepared by
Sandia National Laboratories
Albuquerque, New Mexico 87185 and Livermore, California 94550

Sandia is a multiprogram laboratory operated by Sandia Corporation,
a Lockheed Martin Company, for the United States Department of Energy's
National Nuclear Security Administration under Contract DE-AC04-94AL85000.

Approved for public release; further dissemination unlimited.

TL022917

SANDIA NATIONAL
LABORATORIES
TECHNICAL LIBRARY

Sandia National Laboratories

Issued by Sandia National Laboratories, operated for the United States Department of Energy by Sandia Corporation.

NOTICE: This report was prepared as an account of work sponsored by an agency of the United States Government. Neither the United States Government, nor any agency thereof, nor any of their employees, nor any of their contractors, subcontractors, or their employees, make any warranty, express or implied, or assume any legal liability or responsibility for the accuracy, completeness, or usefulness of any information, apparatus, product, or process disclosed, or represent that its use would not infringe privately owned rights. Reference herein to any specific commercial product, process, or service by trade name, trademark, manufacturer, or otherwise, does not necessarily constitute or imply its endorsement, recommendation, or favoring by the United States Government, any agency thereof, or any of their contractors or subcontractors. The views and opinions expressed herein do not necessarily state or reflect those of the United States Government, any agency thereof, or any of their contractors.

Printed in the United States of America. This report has been reproduced directly from the best available copy.

Available to DOE and DOE contractors from
U.S. Department of Energy
Office of Scientific and Technical Information
P.O. Box 62
Oak Ridge, TN 37831

Telephone: (865) 576-8401
Facsimile: (865) 576-5728
E-Mail: reports@adonis.osti.gov
Online ordering: http://www.osti.gov/bridge

Available to the public from
U.S. Department of Commerce
National Technical Information Service
5285 Port Royal Rd.
Springfield, VA 22161

Telephone: (800) 553-6847
Facsimile: (703) 605-6900
E-Mail: orders@ntis.fedworld.gov
Online order: http://www.ntis.gov/help/ordermethods.asp?loc=7-4-0#online

SAND2007-2319
Unlimited Release
Printed March 2008

Experiments for Calibration and Validation of Plasticity and Failure Material Modeling: 6061-T651 Aluminum

Sam X. McFadden and John S. Korellis
Mechanics of Materials Department
Mail Stop 9049

Ken L. Lee
Analytical Materials Science Department
Mail Stop 9161

Sandia National Laboratories
P.O. Box 969
Livermore, CA 94551-0969

Brendan R. Rogillo and Paul W. Hatch
Experimental Environment and Test Simulation Department
Sandia National Laboratories
P.O. Box 5800
Albuquerque, NM 87185-0555

Abstract

Experimental data for material plasticity and failure model calibration and validation were obtained from 6061-T651 aluminum, in the form of a 4-in. diameter extruded rod. Model calibration data were taken from smooth tension, notched tension, and shear tests. Model validation data were provided from experiments using thin-walled tube specimens subjected to path-dependent combinations of internal pressure, extension, and torsion.

ACKNOWLEDGEMENTS

Mike Chiesa performed preliminary validation test simulations and provided a validation test matrix containing path-dependent combinations of pressure, rotation, and axial displacement. Sangwok (Simon) Lee assisted with the validation tests in CA.

CONTENTS

1. Introduction 7

2. Experimental details 9
   2.1. Calibration tests 9
   2.2. Validation experiments 12
   2.3. Test frames and instrumentation 14
   2.4. Measurement accuracy and precision 16

3. Results 17
   3.1. Calibration data 17
   3.2. Validation data 24
      3.2.1. Load path 1: pressure only 26
      3.2.2. Load path 2: stroke only 28
      3.2.3. Load paths 3 through 6: rotation and stroke 30
      3.2.4. Load paths 7 and 8: pressure, rotation, and stroke 38
      3.2.5. Load path 9: pressure and rotation 42
      3.2.6. Load path 10: pressure and stroke 44
      3.2.7. Machine compliance 45

4. Comments 49

5. References 51

Appendix A: Material certification 6061-T651 53

Appendix B: Smooth tension specimen gage profiles 55

TABLES

Table 1. Tensile specimen nominal dimensions. 11
Table 2. Specimen type, test temperature, and displacement rate. 12
Table 3. Validation tests. 14

FIGURES

Figure 1. Examples of raw stock after specimen extraction. 10
Figure 2. Tensile specimens. 10
Figure 3. Raw stock showing shear specimen extraction. 11
Figure 4. Shear specimen and fixture ready for testing. 11
Figure 5. Validation test specimen geometry. 13
Figure 6. Axial, radial, rotational displacement gage. 15
Figure 7. Validation specimen and displacement gage. 16
Figure 8. Smooth tension data (–65°F). 17
Figure 9. Smooth tension data (70°F). 18
Figure 10. Smooth tension data (165°F). 19
Figure 11. Notched tension data (70°F). 20
Figure 12. Notched tension (165°F). 21
Figure 13. Smooth tension data, radial position longitudinal orientation, and transverse orientation comparison (70°F). 22
Figure 14. Shear stress-strain data (70°F). 23
Figure 15. Shear load-displacement data (70°F). 24
Figure 16. Schematic representation of the difference between rotation- and angular-displacement measurements. 25
Figure 17. Load path 1 data (tube 1). 26
Figure 18. Post-test images of load path 1 specimen (tube 1). 27
Figure 19. Load path 2 data (tube 3). 28
Figure 20. Post-test images of load path 2 specimen (tube 3). 29
Figure 21. Load path 3 data (tube 7). 30
Figure 22. Post-test images of load path 3 specimen (tube 7). 31
Figure 23. Load path 4 data (tube 4). 32
Figure 24. Post-test images of load-path 4 specimen (tube 4). 33
Figure 25. Load path 5 data (tube 8) 34
Figure 26. Post-test images of load path 5 specimen (tube 8). 35
Figure 27. Load path 6 data (tube 9). 36
Figure 28. Post-test images of load path 6 specimen (tube 9). 37
Figure 29. Load path 7 data (tube 2). 38
Figure 30. Post-test images of load path 7 specimen (tube 2). 39
Figure 31. Load path 8 data (tube 11). 40
Figure 32. Post-test images of load path 8 specimen (tube 11). 41
Figure 33. Load path 9 data (tube 12). 42
Figure 34. Post-test images of load path 9 specimen (tube 12). 43
Figure 35. Load path 10 data (tube 6). 44
Figure 36. Post-test images of load path 10 specimen (tube 6). 45
Figure 37. Axial compliance data. 46
Figure 38. Torsional compliance data. 47

1. INTRODUCTION

This work was conducted to provide the experimental basis for calibration and validation of metal plasticity and failure models. The aluminum alloy 6061-T651 was selected as a structural material of general interest to Sandia. Although 6061 aluminum has been extensively characterized, ongoing model application and development efforts require complete stress-strain or load-displacement histories from a range of specimen geometries and test conditions. Such data is not generally available. Therefore, significant laboratory work is required to provide the necessary basis for modeling plasticity and failure, even for common alloys such as 6061. Much of the data presented here have been entered into the Materials Weapon Information System and Data Management application (WISDM) [1].

Raw stock was purchased in the form of 4-in. diameter extruded rod produced by Alcoa. Material certification is included in Appendix A. All specimens used for this study were extracted from the same lot of material. Constitutive model calibration data were obtained from smooth tension, notched tension, and shear tests. Not all material models in use at Sandia require each of these specimen geometries for calibration. However, if a specimen geometry is not needed for calibration, the data may be used to verify calibration or as first-level validation. Validation data were obtained using thin-walled tube specimens subjected to complex stress and strain states through the application of internal pressure combined with axial and torsional loading. The specimen geometry and loading conditions did not support principal stresses or strains normal to the specimen surface. Consequently, the stress and strain states covered a range of biaxial conditions. Because each of the three actuators (axial, torsional, and pressure) were operated under closed-loop control, it was possible to explore the path dependence of plasticity and failure over a wide range of loading conditions.

This page intentionally left blank.

2. EXPERIMENTAL DETAILS

2.1. Calibration tests

Tensile specimens were extracted from 2.646-in. and 1.356-in. diameter circles with respect to the center of the 4-in. diameter rod, oriented with the tensile axis parallel to the extrusion direction. A limited number of smooth tension specimens were prepared to show the affect of radial position within the rod on tensile behavior by extracting specimens along 1.074-in., 2.148-in., and 3.222-in. diameter circles with respect to the rod center. Mechanical property anisotropy was demonstrated by testing smooth tension specimens extracted transverse to the rod axis 0.5 in. from the rod center. However, since the material models currently in use at Sandia do not handle anisotropy, a complete characterization of the transverse properties was not performed. Examples of raw stock after specimen extractions are shown in Figure 1. The nominal dimensions of tensile specimens used in this work are listed in Table 1, and examples are shown in Figure 2. The notched tension specimen design has been used extensively for investigation of the damage parameters that are part of the BCJ and EMMI material models. To promote failure within the gage length, it is common practice to machine smooth tension specimens with a diameter that is .001 to .003 in. larger at the ends of the gage section than in the center. However, because of the low work hardening of 6061 aluminum, the ultimate strain and total elongation are sensitive to dimensional changes within the gage length. Consequently, measurements were made at ten locations along the gage length of each smooth tension specimen to document the gage profile. The profile data are included in Appendix B. The specimen numbers listed in Appendix B correspond to the specimen numbers noted on the data plots in the results section of this report, and in the data files found in WISDM [2]. Displacement was measured over a 1.0-in. gage length for all of the tension tests.

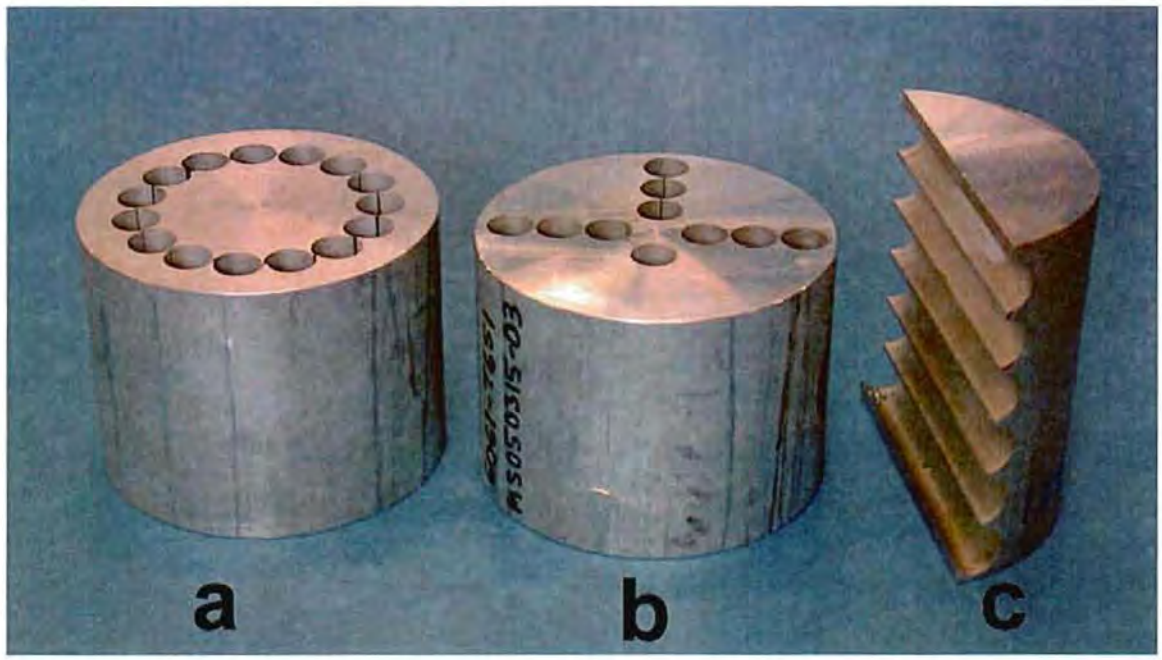

Figure 1. Examples of raw stock after specimen extraction. The majority of smooth and notched tension specimens were extracted from a 2.646-in. diameter circle (a). The influence of radial position within the rod on tensile behavior (b) and the transverse smooth tension properties (c) were investigated.

Figure 2. Tensile specimens. From left to right: notched R1, R2, R4, and smooth.

Table 1. Tensile specimen nominal dimensions.

Specimen	Gage diameter (in.)	Shoulder diameter (in.)	Notch radius (in.)
Smooth	0.250	NA	NA
R1	0.250	0.5	0.039
R2	0.250	0.5	0.078
R4	0.250	0.5	0.390

Shear properties were obtained using a v-groove specimen geometry and commercial test fixture consistent with ASTM D 5379-05 [3]. While this standard was written for composite materials, the specimen geometry and test fixture were originally developed by Iosipescu to investigate shear in metals [4]. The shear specimens were extracted with the shear plane oriented at 45° to the rod axis, so as to complement the principal shear planes in the tensile tests. The specimens were located between 0.350 in. and 0.850 in. from the rod center. The nominal gage length and thickness were 0.450 and 0.090 in., respectively. Figure 3 shows the shear specimen extraction orientation with respect to the 4-in. diameter rod. Strain gages were bonded to the specimens for determination of shear strain in the small strain region. Typically, material model (EMMI) shear term calibration is performed by fitting load-displacement data. The relative displacement of the two halves of the shear fixture was measured with a linear displacement gage, and corrected for test fixture compliance. A shear specimen and fixture ready for testing is shown in Figure 4.

Figure 3. Raw stock showing shear specimen extraction.

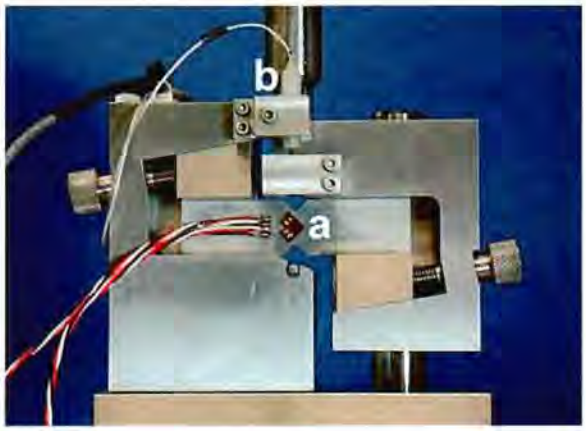

Figure 4. Shear specimen and fixture ready for testing. Strain gages are bonded to the specimen at ±45° to the shear plane (a). The right half of the fixture is displaced downward with respect to the left half. A DVRT (b) measures the relative displacement.

Calibration tests were run under conducted at two rates and at three different temperatures. Table 2 contains the matrix of specimen type, temperature, and rate. The 0.002 in./s tests were conducted under closed loop constant displacement rate control, while the 10 in./s rate tests were run under open loop displacement rate control.

Table 2. Specimen type, test temperature, and displacement rate.

		Nominal displacement rate Displacement rate (in./s)	
Specimen	**Temperature (°F)**	**0.002**	**10**
Smooth tension	–65	X	
	70	X	X
	165	X	X
Notched tension R1	–65		
	70		X
	165		X
Notched tension R2	–65		
	70		X
	165		X
Notched tension R4	–65		
	70		X
	165		X
Shear	–65		
	70	X	
	165		

2.2. Validation experiments

The model validation specimen geometry is shown in Figure 5. The specimens were extracted with centers located 1.0 in. from the rod center. Measurements of the as-machined specimen inner diameters (ID) showed an average of 0.8759 in. with a standard deviation of 0.0002 in. Measurements of the as-machined specimen gage section outer diameters (OD) showed an average of 0.9998 in., with a standard deviation of 0.0001 in. Each of the servo-hydraulic actuators that controlled pressure, extension, and rotation were operated under closed loop control. In this paper, "stroke" is used to denote actuator axial displacement, and "rotation" is used to denote actuator rotational displacement. To simplify the model boundary conditions that would correspond to each experiment, test frame control signals were restricted to stroke, rotation, and pressure.

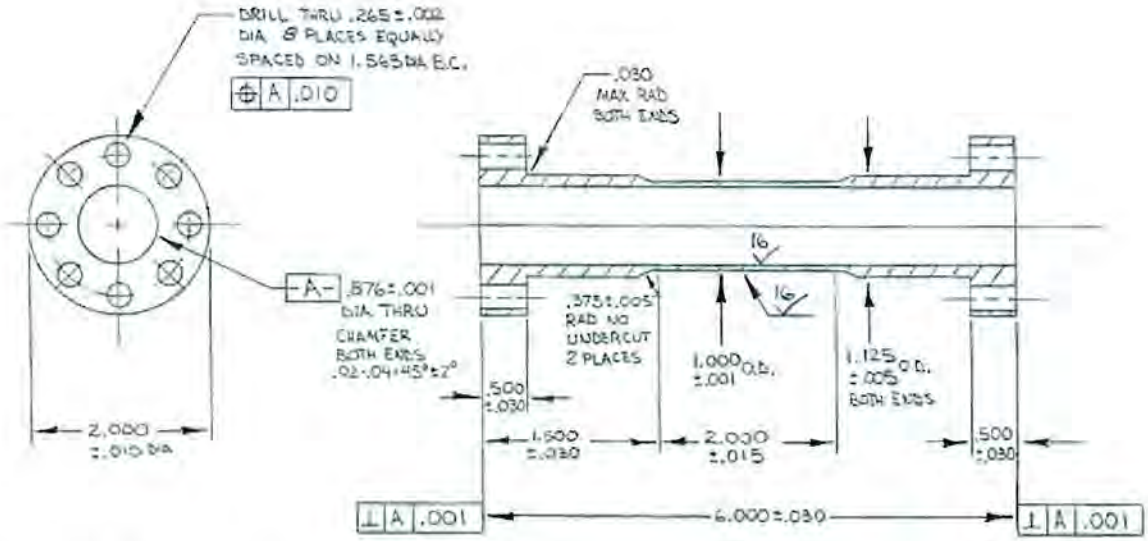

Figure 5. Validation test specimen geometry.

Because the stroke and rotation data contained load frame displacements in addition to specimen displacements, the load frame compliance was measured by mounting a solid steel link in place of a validation test specimen. The steel link geometry was similar to the validation specimens, but the diameter was 1.125 in., and the length between flanges was 2.5 in. The axial and torsional loads were independently ramped, and the stroke and rotation signals were recorded with the loads. By comparing measured stroke and rotation to calculated elastic deflection of the solid link, load frame compliance may be accounted for when comparing simulations to the experimental data.

The validation test matrix is shown in Table 3. Each step shown in the table was run sequentially, and the indicated signal was controlled with a linear ramp to the specified level. At the end of each step, the indicated signal was held constant at the specified level. For example, in load path 7, step 1, the pressure was ramped to 2500 psi while the rotation and stroke were held at 0° and 0 in. In step 2, the pressure was held constant at 2500 psi while the rotation was ramped to 30° and the stroke was held at 0 in. In step 3, the pressure and rotation were maintained at 2500 psi and 30°, while the stroke was ramped until specimen failure. Pressure was ramped at rates between 10 and 37 psi/s. Rotation was ramped at 0.25 °/s, and stroke was ramped between 0.0005 and 0.001 in./s. Because of the strain rate insensitivity of 6061 aluminum, the variations in ramp rates had insignificant effects on the validation data. All validation tests were conducted at laboratory temperature (70°F).

Table 3. Validation tests.

Load path	Step 1	Step 2	Step 3	Tube
1	Rotation 0	Stroke 0	Pressure to failure	1
2	Pressure 0	Rotation 0	Stroke to failure	3
3	Pressure 0	Rotation to 30°	Stroke to failure	7
4	Pressure 0	Rotation to 85°	Stroke to failure	4
5	Pressure 0	Torque 2500 in.-lb†	Stroke (not to failure)	8
6	Pressure 0	Axial strain 0.04*	Rotation to limit	9
7	Pressure 2500 psi	Rotation 30°	Stroke to failure	2
8	Pressure 5000 psi	Rotation 30°	Stroke to failure	11
9	Stroke 0	Pressure to 5000 psi	Rotation to failure	12
10	Rotation 0	Pressure 2500 psi	Stroke to failure	6

†Step 2 was run in rotation control to a torque level of 2500 in.-lb, followed by a control mode switch to constant torque of 2500 in.-lb during step 3. The experiment ended before failure in stoke when the rotational actuator reached its physical limit.
*Step 2 was run in stroke control to the axial displacement gage signal level of 0.04 in. Stroke was then held constant during step 3, rotation to failure.

2.3. Test frames and instrumentation

All tests were completed on MTS servo-hydraulic load frames. Calibration tests run at 0.002 in./s were controlled and data recorded with MTS TestStar Classic hardware and software. Force was measured with standard MTS load cells, and tension test displacements were measured with 1.0-in. gage length MTS extensometers. The linear displacement gage used to measure shear fixture displacement was a differential variable reluctance transducer (DVRT) and conditioner manufactured by MicroStrain. Strain gages bonded to the shear specimens had a gage length of 0.032 in., and the signals were processed with Vishay model 2311 conditioners, which provided analog output to the TesStar controller.

The 10 in./s calibration tests were operated with MTS 458.20 controllers and signal conditioning, while data was recorded with a Nicolet 440 or 40 Pro digital oscilloscope. Loads for the 10 in./s tests were measured with a 50 kip Kistler quartz load washer and Kistler Model 5010B charge amplifier. Smooth tension specimen displacements were measured with 1.0-in. gage length MTS extensometers. Notched tension displacements were measured over a 1.0-in. gage length with a Fotonics optical displacement sensor, or a MicroStrain DVRT.
An ATS environmental chamber and Barber-Coleman process controller were employed for maintaining test temperatures of 165°F and –65°F using electric resistance heating

and liquid nitrogen cooling. Temperature feedback was provided by a type K thermocouple held in contact with the specimen using seizing wire.

The complex loading validation tests were completed on a MTS load frame with 100 kip axial and 50 kip torsional capacity. Specimen internal pressure was provided by a MTS 286.50 pressure intensifier, which used a servo-hydraulic ram to pressurize and control water that was fed into the test fixture. Pressure was measured near the inlet port to the specimen, with a 10 ksi transducer and TestStar DC signal conditioner. The axial, torsional, and pressure actuators were controlled with TestStar Classic hardware and software. Axial, radial, and rotational displacements were measured on the specimen using the displacement gage shown in Figure 6 [5]. The gage employed LVDTs and RVDTs. The signals were processed with three TestStar AC conditioners. The axial displacement gage length of 1.0 in. was determined by the distance between the locator pins in the assembly. Figure 7 shows the extensometer mounted on a specimen.

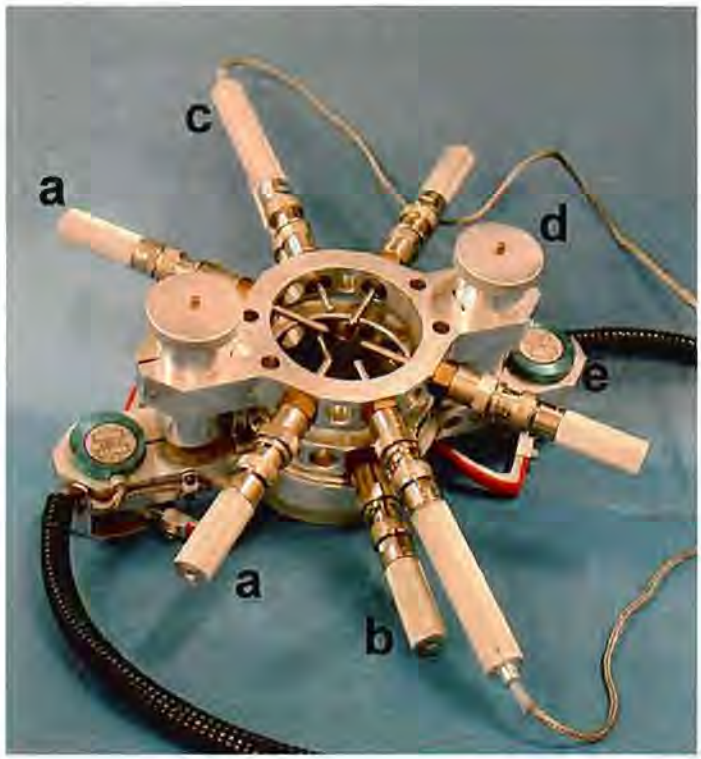

Figure 6. Axial, radial, and rotational displacement gage. The gage fits around the validation specimen. Two pairs of conical tip spring loaded contact pins (a) fix the top half of the gage to the specimen, while one pair (b) fixes the bottom half, with 1.0 in. of vertical separation (gage length). Two similar opposing pins in the top half (c) contain LVDTs that measure radial displacement. Axial displacement is obtained from two LVDTs (d) that measure the displacement between the upper and lower sets of contact pins. Rotational displacement is obtained from two RVDTs (e) that measure the angular difference between the upper and lower sets of contact pins. The signal from each pair of LVDTs and RVDTs is summed to provide an average displacement.

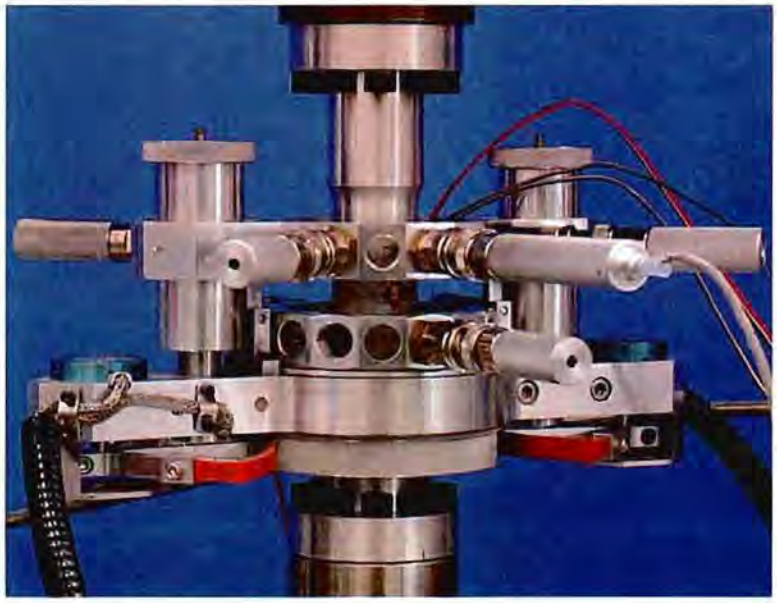

Figure 7. Validation specimen and displacement gage.

2.4. Measurement accuracy and precision

The measurement accuracy and precision of this work was established by load and displacement transducers calibrated in accordance with industry standards using measurement values traceable to the National Institute of Standards and Technology (NIST). The MTS LVDTs and RVDTs, integral to the load frames, were calibrated in accordance with MTS Procedure FS-CA 2104 Rev. E. MTS load cells were calibrated in accordance with ASTM E4-03. Error for the calibrations was less than 0.25% of reading, with an uncertainty of ±0.25% for a confidence level of 95%. All sensor and signal conditioning systems not calibrated by MTS were calibrated at time of use by comparison to standards traceable to the National Institute of Standards and Technology.

3. RESULTS

3.1. Calibration data

Calibration data is presented in Figure 8 through Figure 15. The data has been entered into WISDM and can be found through the path Catalog:\Metals\Aluminum Alloys\Aluminum 6061\T651, Test Suite: 6061-T651, 4 in diameter rod. The scatter present in the data is not unusual for aluminum alloys. Shear stress vs. shear strain data is shown in Figure 14. The shear strain was obtained from strain gages. Because strain gages have limited range, the shear stress vs. shear strain curves end before specimen failure.

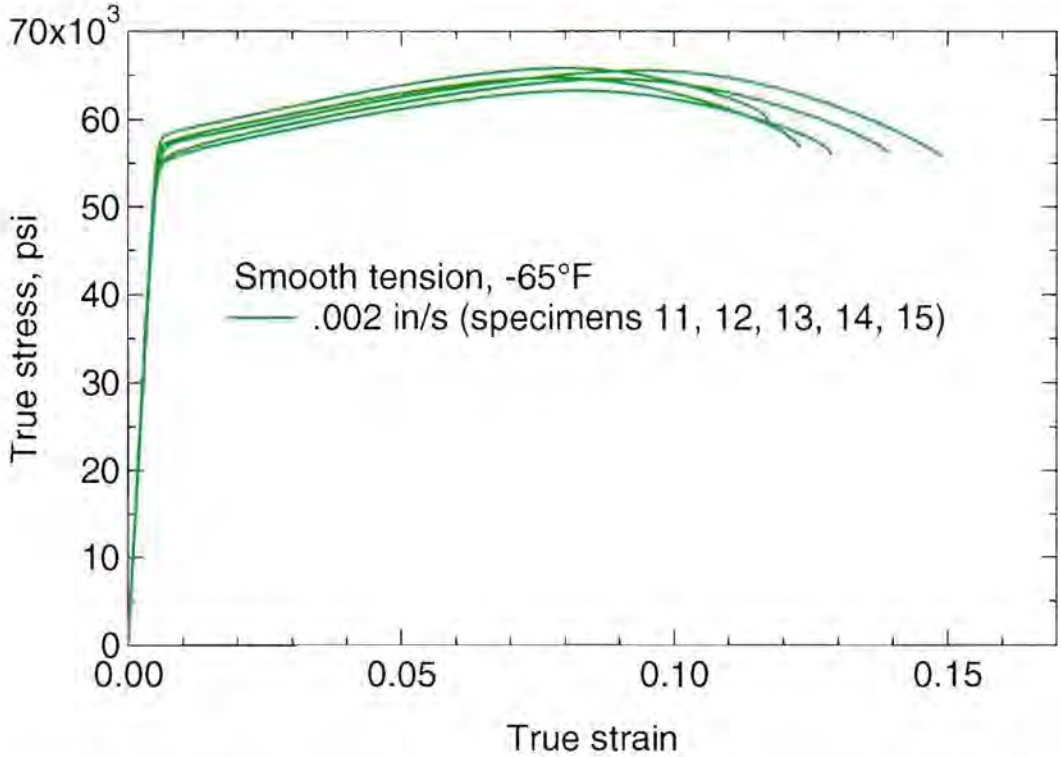

Figure 8. Smooth tension data (–65°F). The specimen numbers correlate to the data in WISDM and the specimen profile measurements in Appendix B.

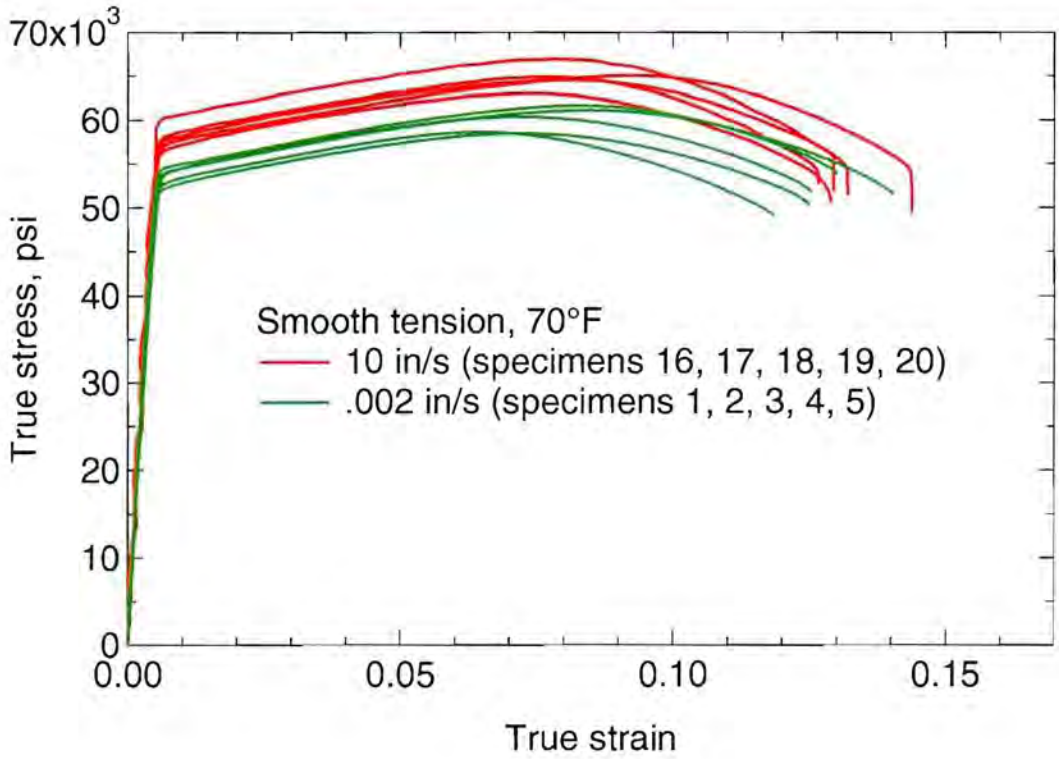

Figure 9. Smooth tension data (70°F). The specimen numbers correlate to the data in WISDM and the specimen profile measurements in Appendix B.

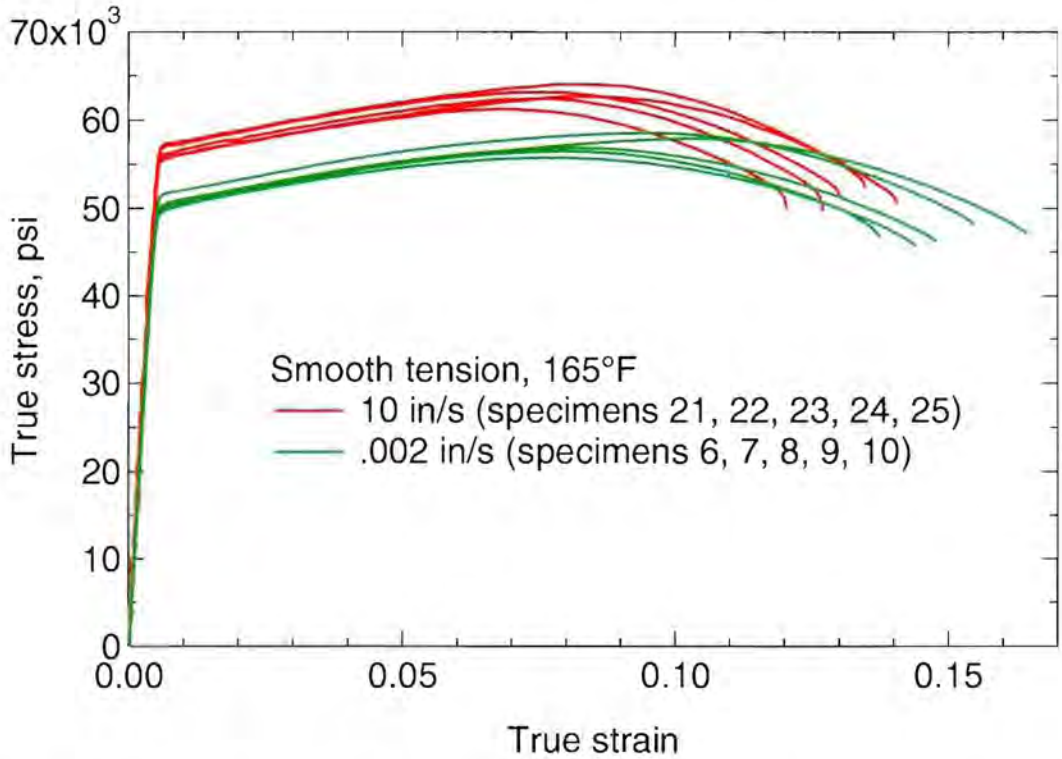

Figure 10. Smooth tension data (165°F). The specimen numbers correlate to the data in WISDM and the specimen profile measurements in Appendix B.

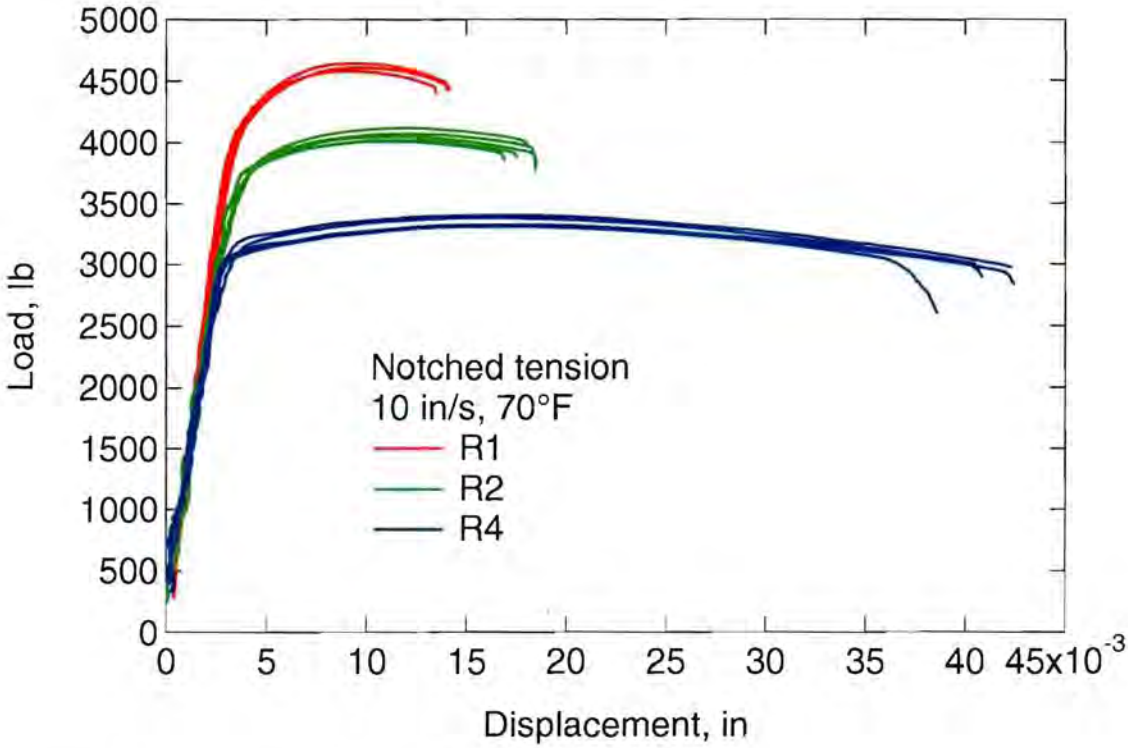

Figure 11. Notched tension data (70°F).

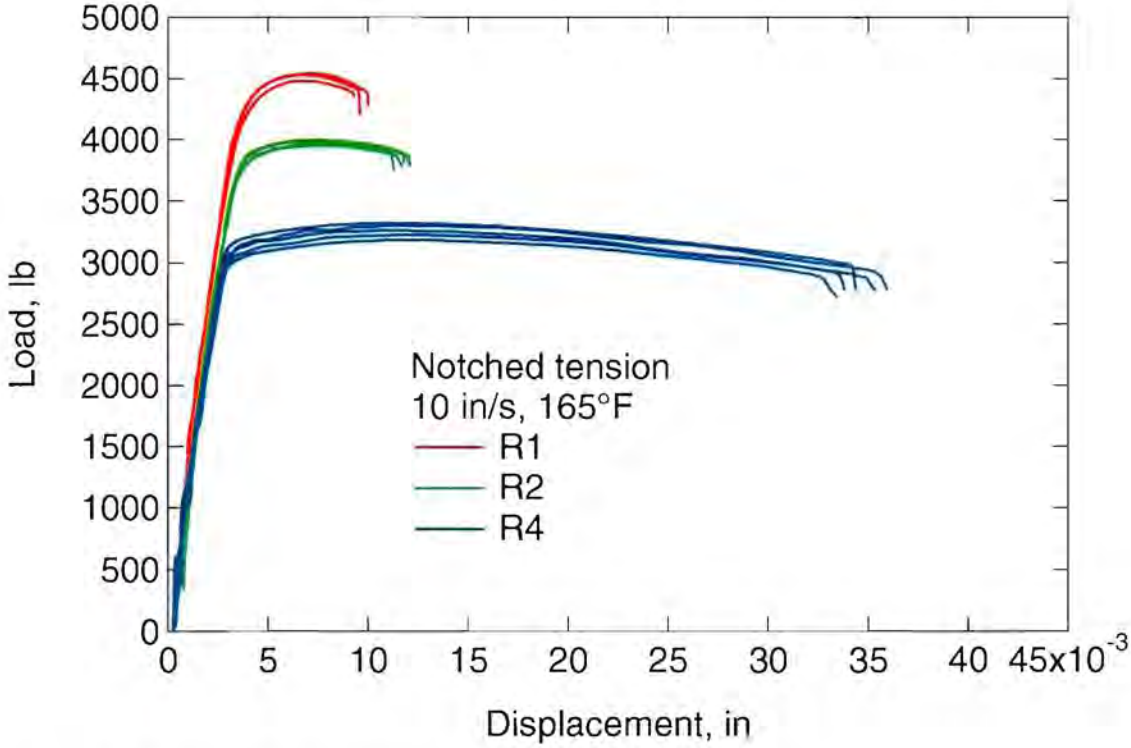

Figure 12. Notched tension (165°F).

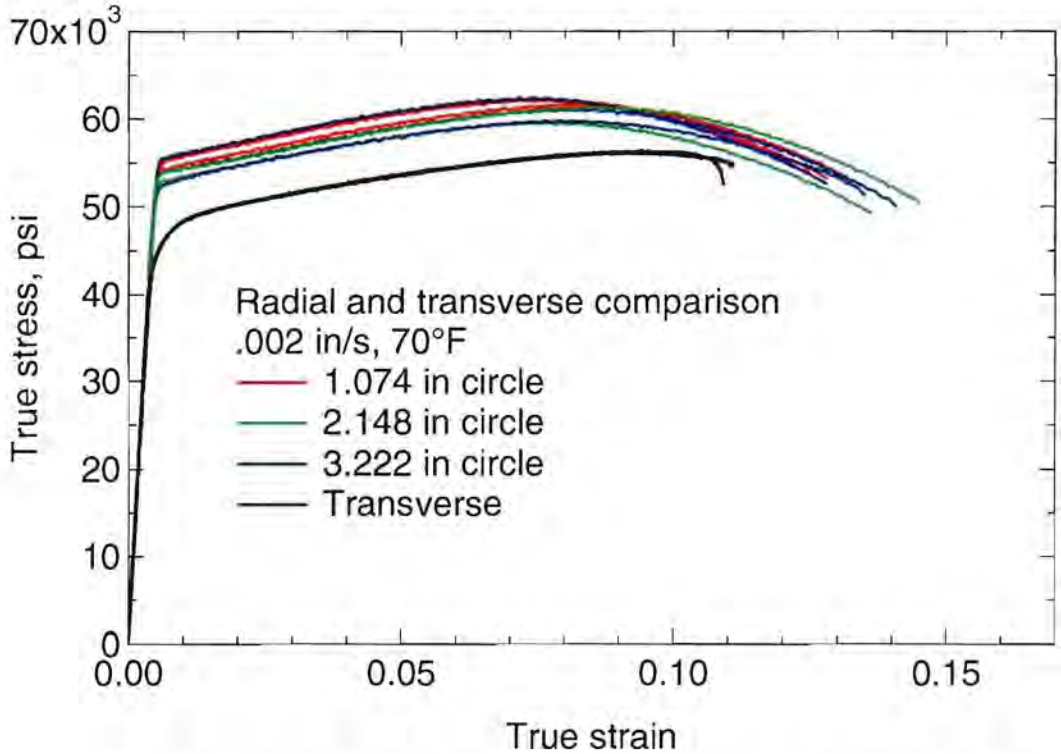

Figure 13. Smooth tension data, radial position longitudinal orientation, and transverse orientation comparison (70°F). Note the very low degree of scatter in the transverse specimen response. The transverse ultimate strains from the extruded rod were larger than the axial ultimate strains, although transverse failure strains were smaller.

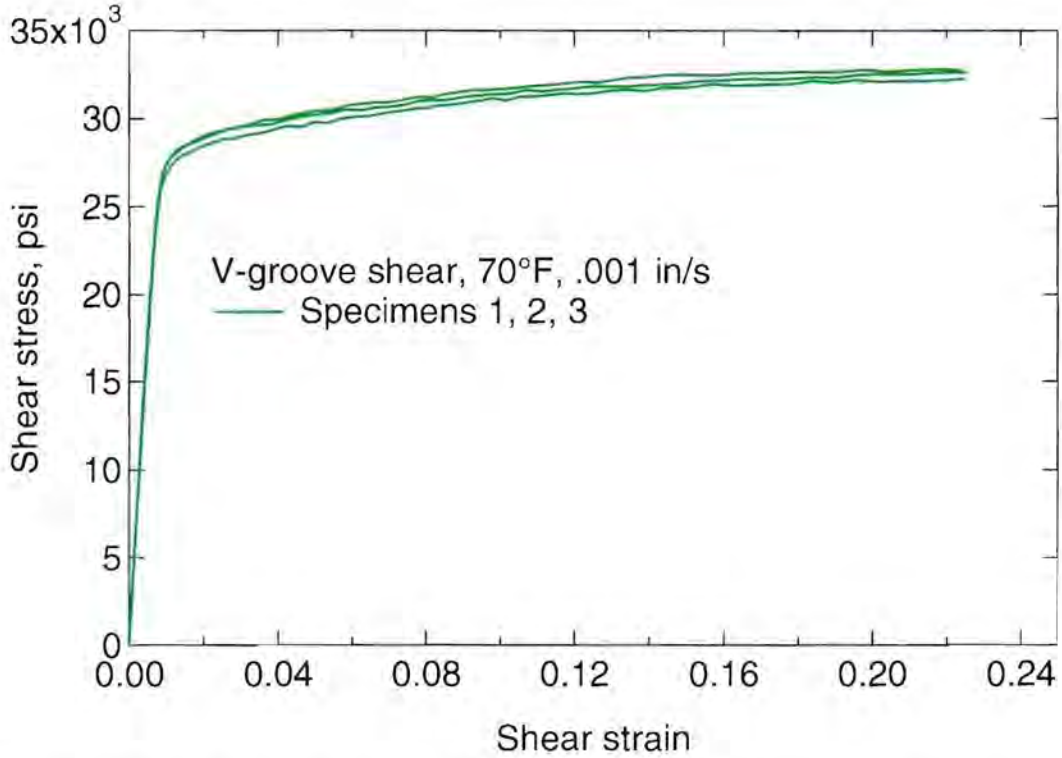

Figure 14. Shear stress-strain data (70°F). Strain data obtained from strain gages. The data show behavior approximately halfway to failure.

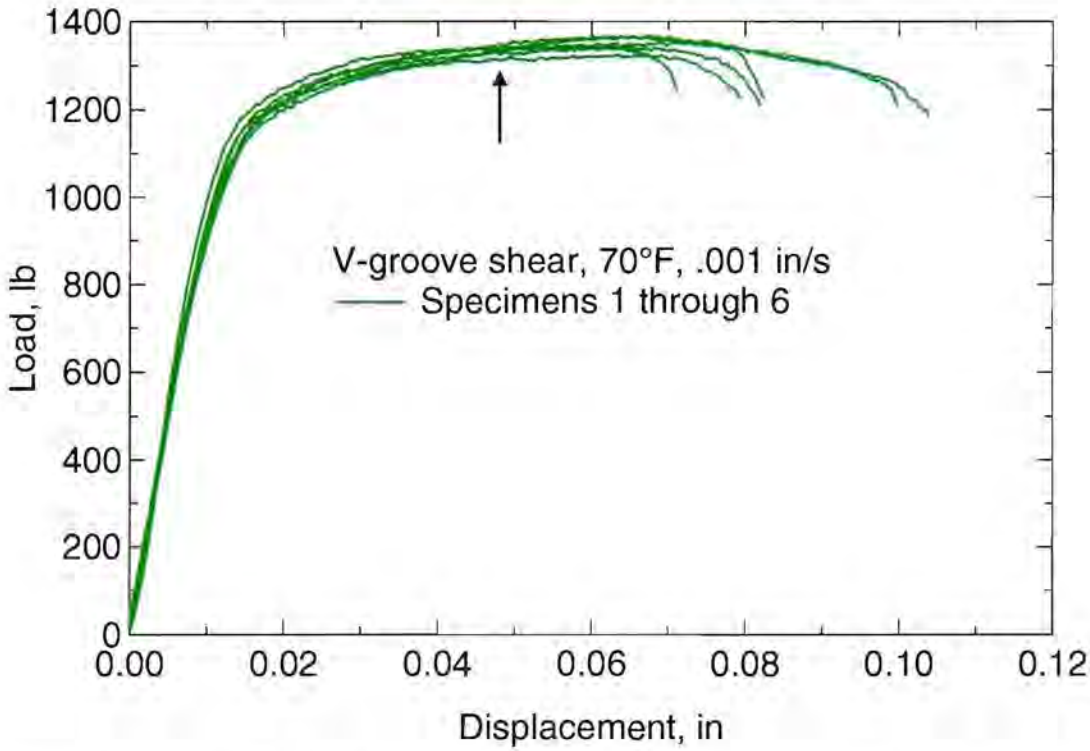

Figure 15. Shear load-displacement data (70°F). Displacement has been corrected for fixture compliance. The arrow indicates the limit of the stress-strain data shown in Figure 14.

3.2. Validation data

The validation test data is presented here as a function of time. Pressure is plotted with diametric displacement. Torque is plotted with rotation and angular displacement. Rotation is a measure of the hydraulic actuator angular position obtained from the load frame RVDT, and angular displacement was measured on the specimen using the displacement gage described previously. Load is plotted with stroke and axial displacement. Stroke is a measure of the hydraulic actuator axial position, and axial displacement was measured on the specimen using the displacement gage described previously. The differences between the rotation and angular displacement measurements and between the stroke and axial displacement measurements are mostly due to the dimensions of the displacement gage, although load frame compliance contributed a small part. The difference between rotation and angular displacement measurement is shown schematically in Figure 16.

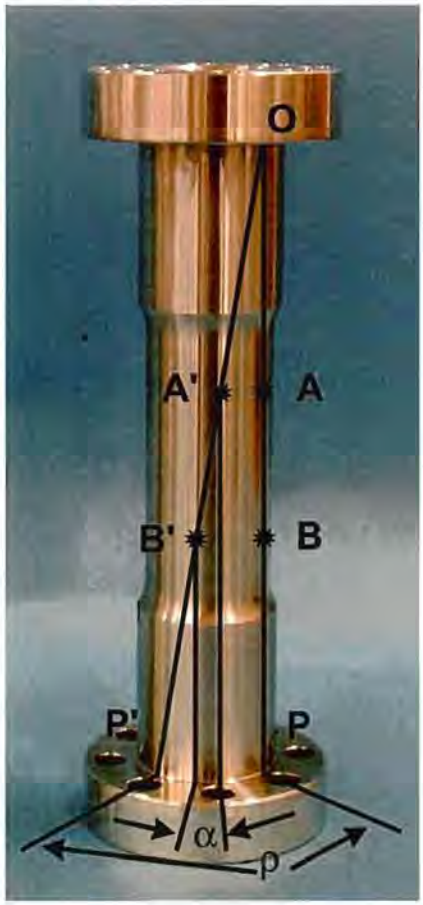

Figure 16. Schematic representation of the difference between rotation- and angular-displacement measurements. The line OP represents a line drawn on the specimen prior to straining in torsion. The line OP' approximates the line OP after straining. Before straining, the upper half of the displacement gage is pinned at A and the lower half is pinned at B. After straining, A is rotated to A', and B is rotated to B'. The angle α is the angle measured by the displacement gage. The angle ρ is the angle measured by the hydraulic actuator RVDT.

3.2.1. Load path 1: pressure only

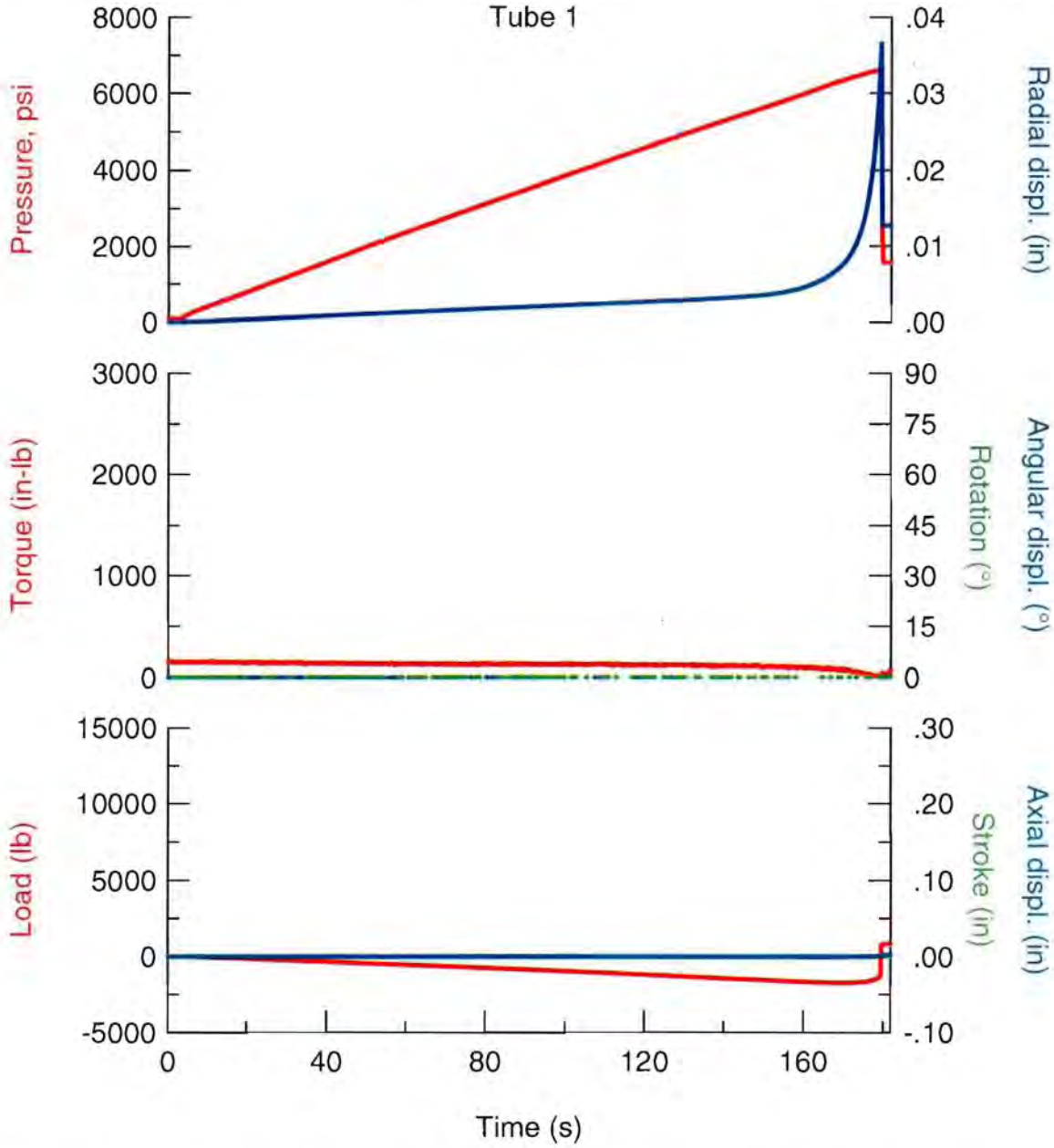

Figure 17. Load path 1 data (tube 1). Rotation and stroke were held at 0° and 0 in., while pressure was ramped to failure. The initial torsional load of 140 in.-lb developed during specimen setup.

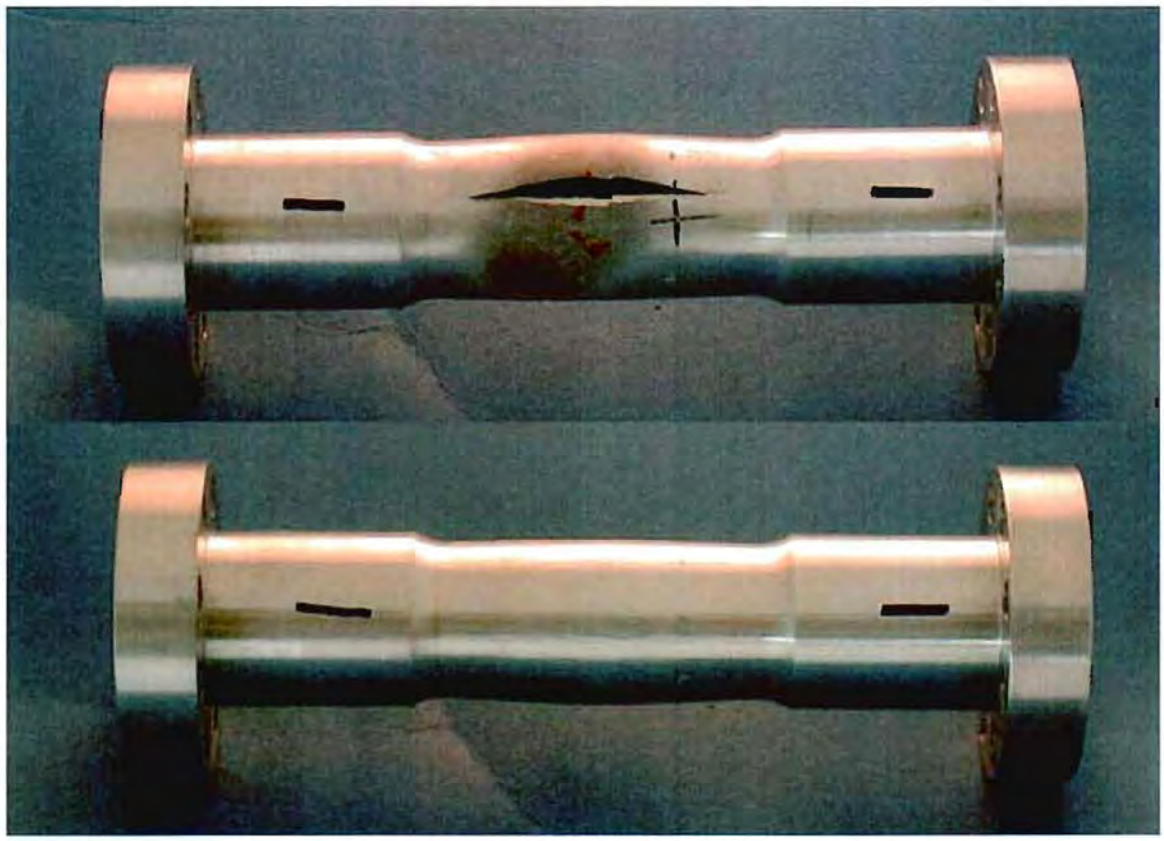

Figure 18. Post-test images of load path 1 specimen (tube 1). The darkened area surrounding the region of failure was caused by microgrit abrasion (25 μm alumina powder) to prepare the surface for strain gages.

3.2.2. Load path 2: stroke only

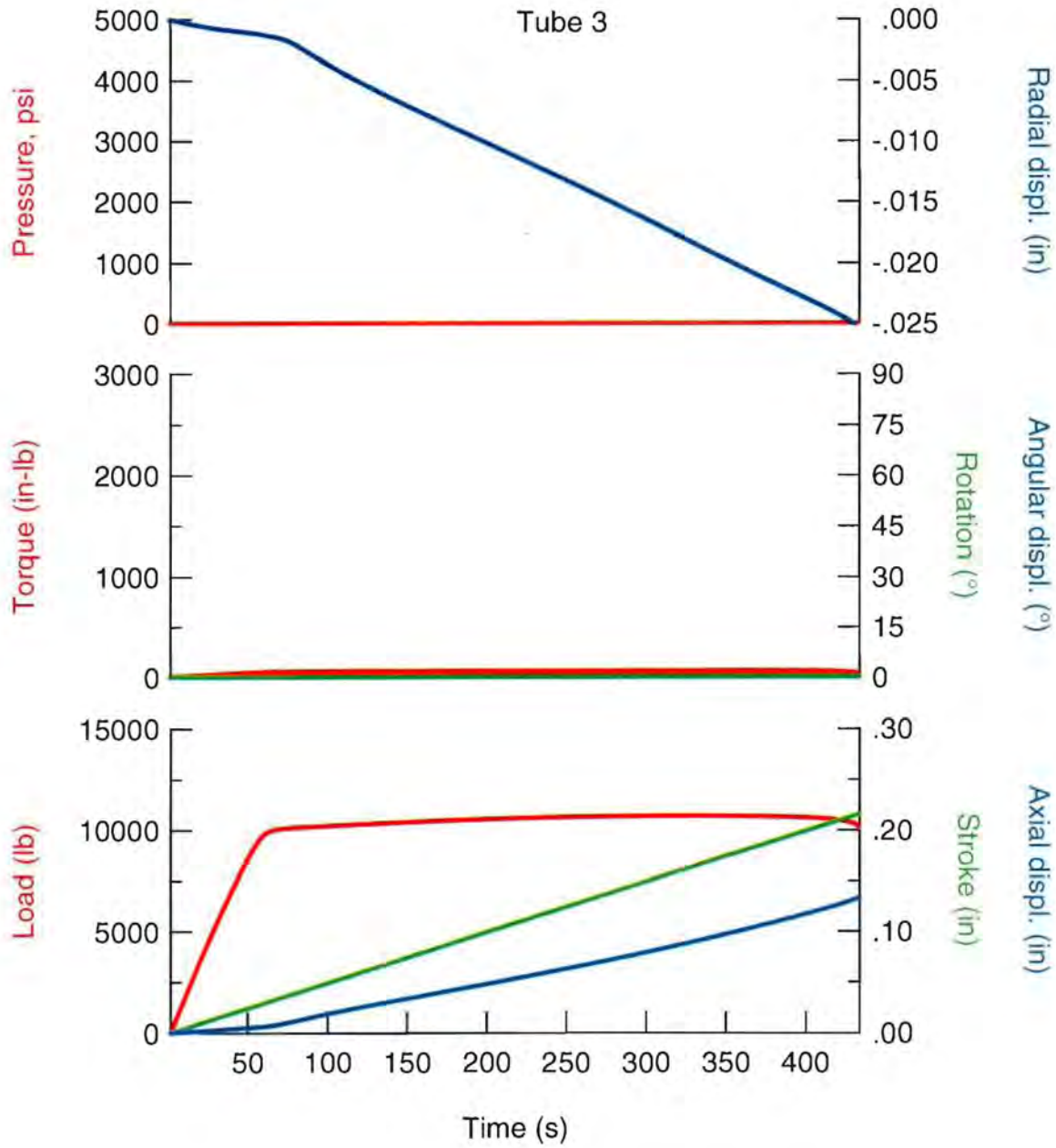

Figure 19. Load path 2 data (tube 3). Pressure and rotation were held at 0 psi and 0°. Stroke was ramped to failure.

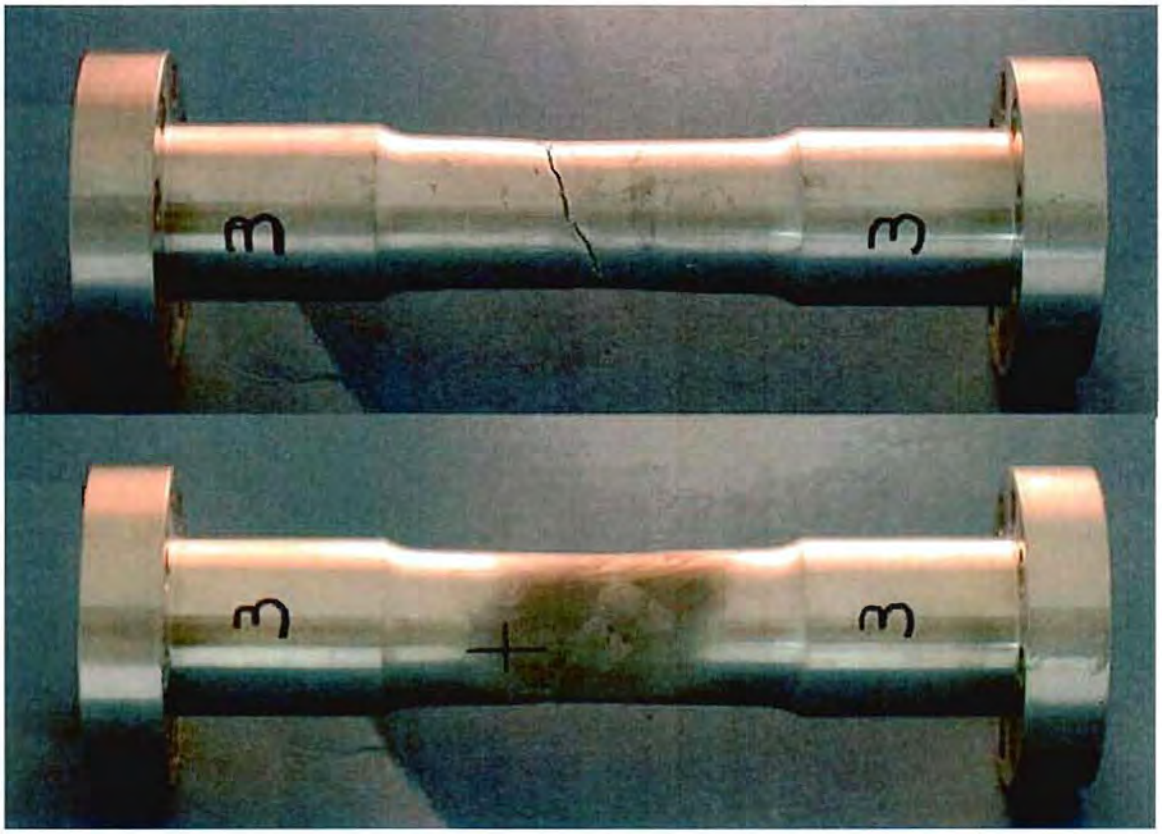

Figure 20. Post-test images of load path 2 specimen (tube 3). Through-wall failure extended to half of the tube circumference.

3.2.3. Load paths 3 through 6: rotation and stroke

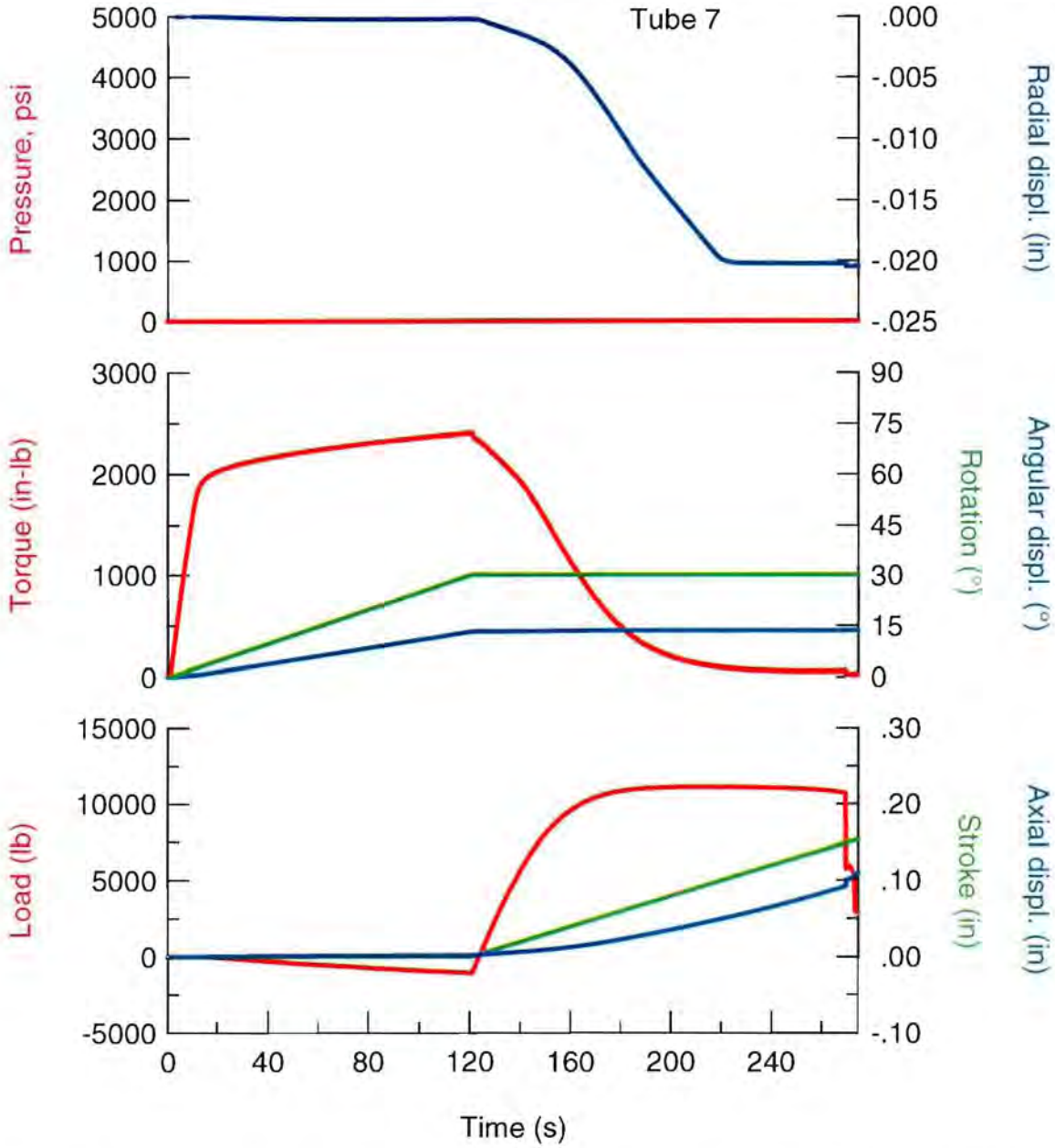

Figure 21. Load path 3 data (tube 7). Pressure was held at 0 psi. Rotation was ramped to 30°, followed by stroke to specimen failure. The diametric displacement gage went out of range during the second half of the stroke step.

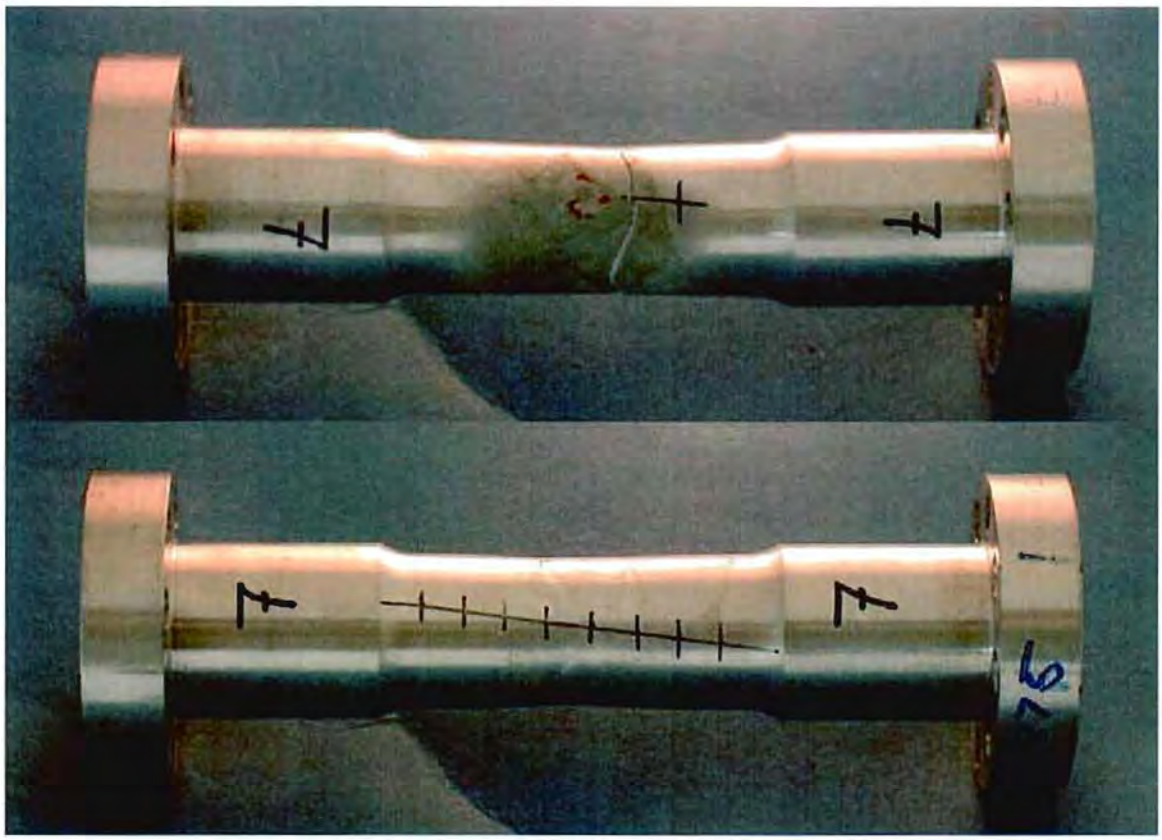

Figure 22. Post-test images of load path 3 specimen (tube 7). The line in the lower image was drawn parallel to the specimen axis prior to deformation. Through-wall failure extended to half of the tube circumference. Necking was visible in regions where failure was not through-wall.

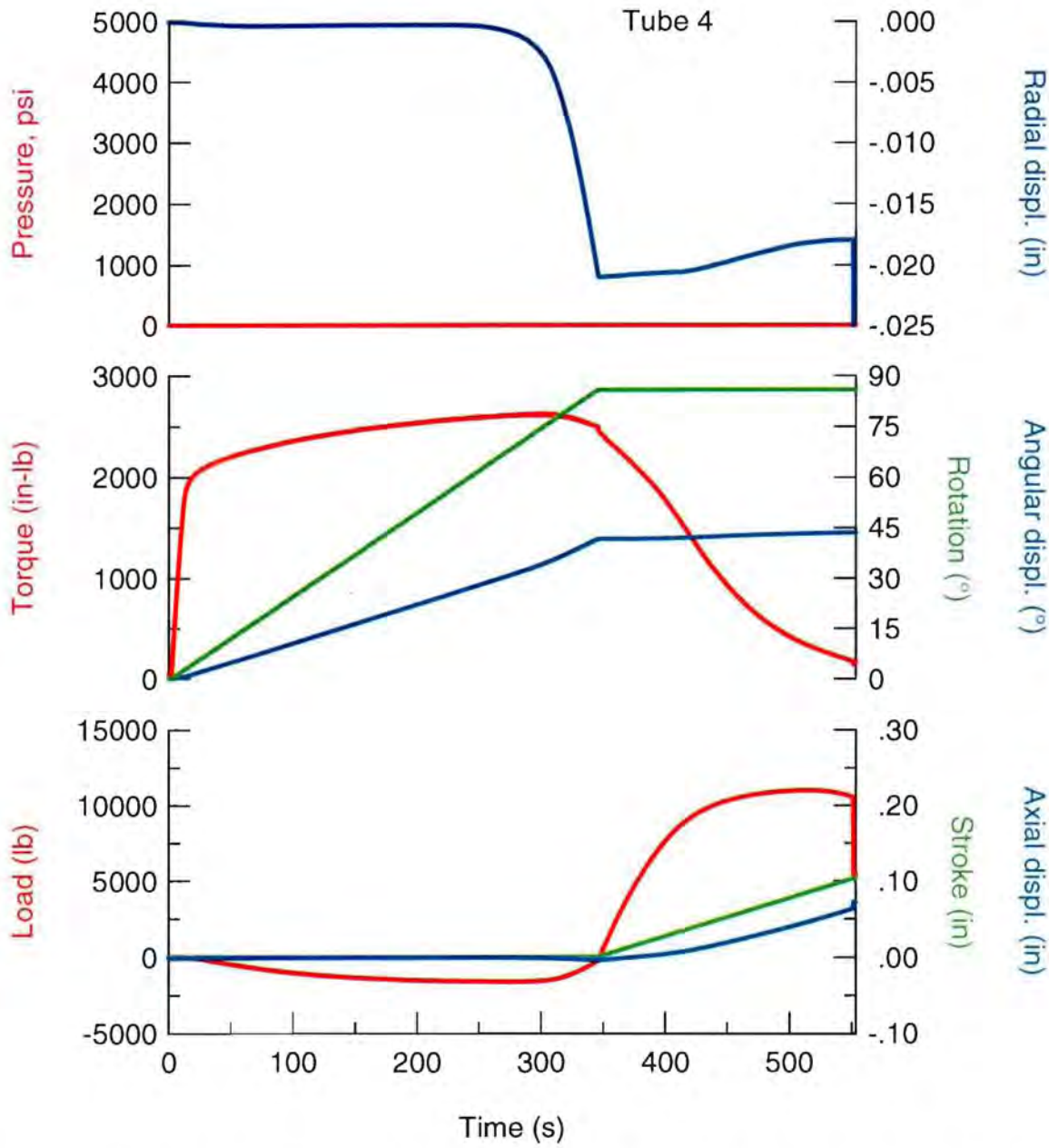

Figure 23. Load path 4 data (tube 4). Pressure was held at 0 psi. Rotation was ramped to 85°, followed by stroke to specimen failure.

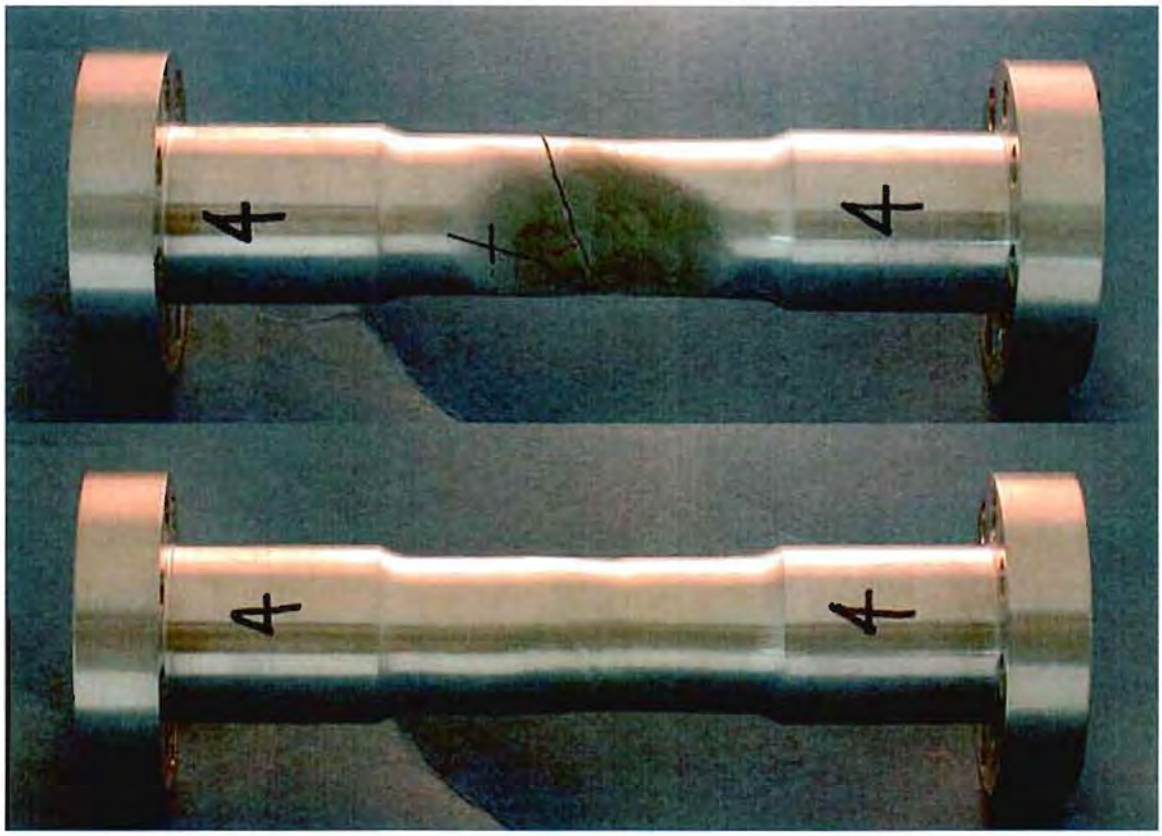

Figure 24. Post-test images of load-path 4 specimen (tube 4). Through-wall failure extended to half of the tube circumference. Necking was visible in regions where failure was not through-wall.

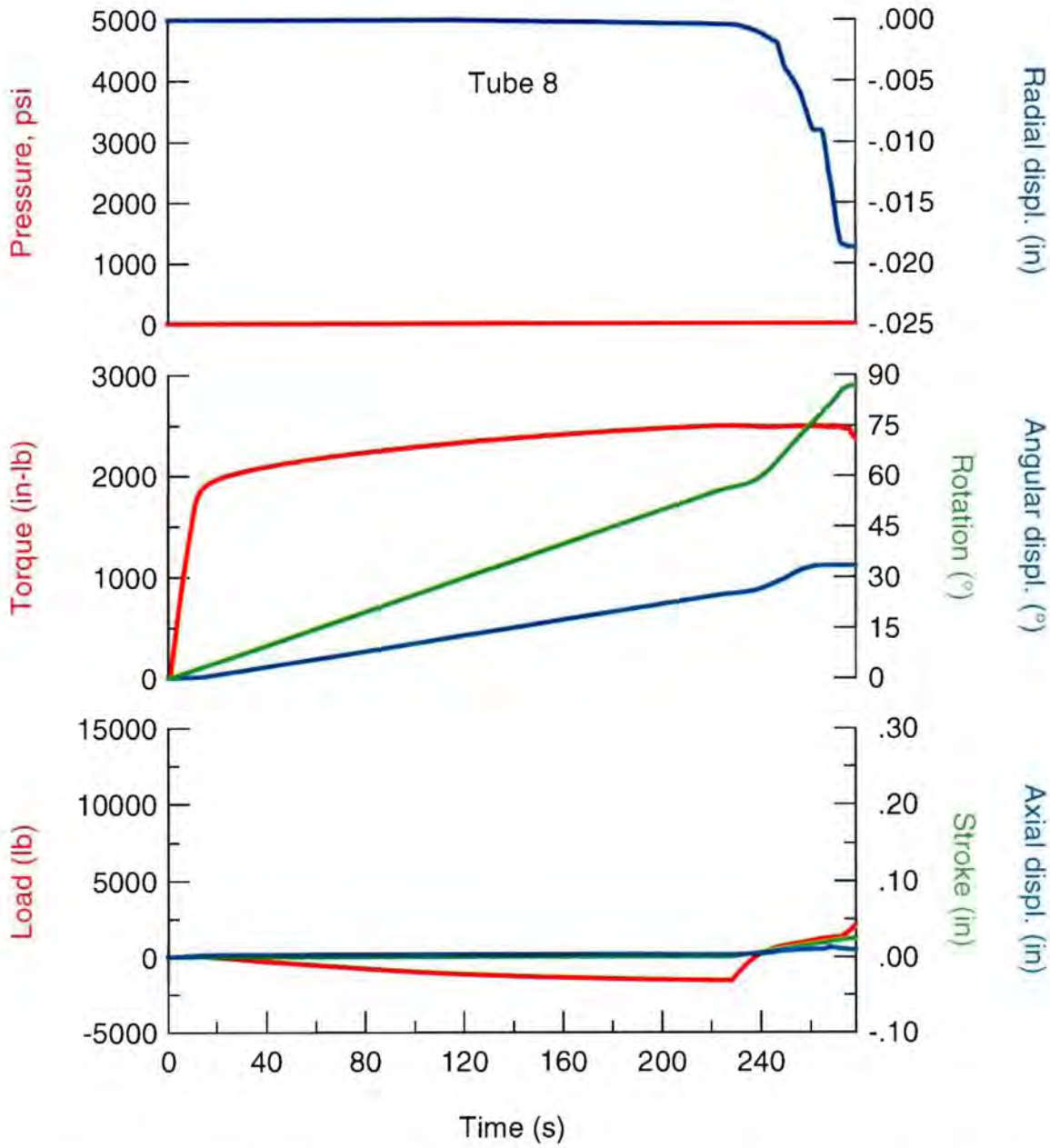

Figure 25. Load path 5 data (tube 8). Pressure was held at 0 psi. Rotation was ramped to a torque of 2500 in-lb, followed by stroke. During the stroke step, the rotation channel was held in torque control at 2500 in-lb. The experiment ended when the rotational actuator reached its physical limit.

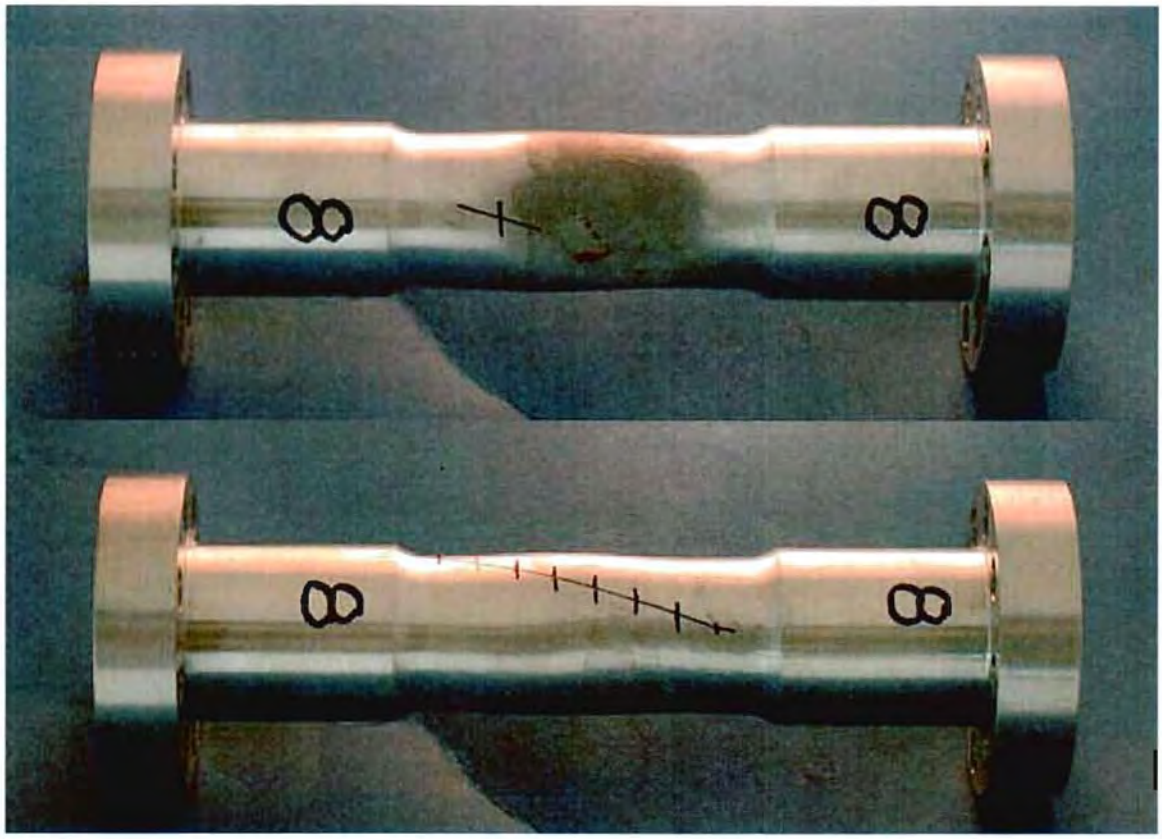

Figure 26. Post-test images of load path 5 specimen (tube 8). The specimen was buckled in torsion.

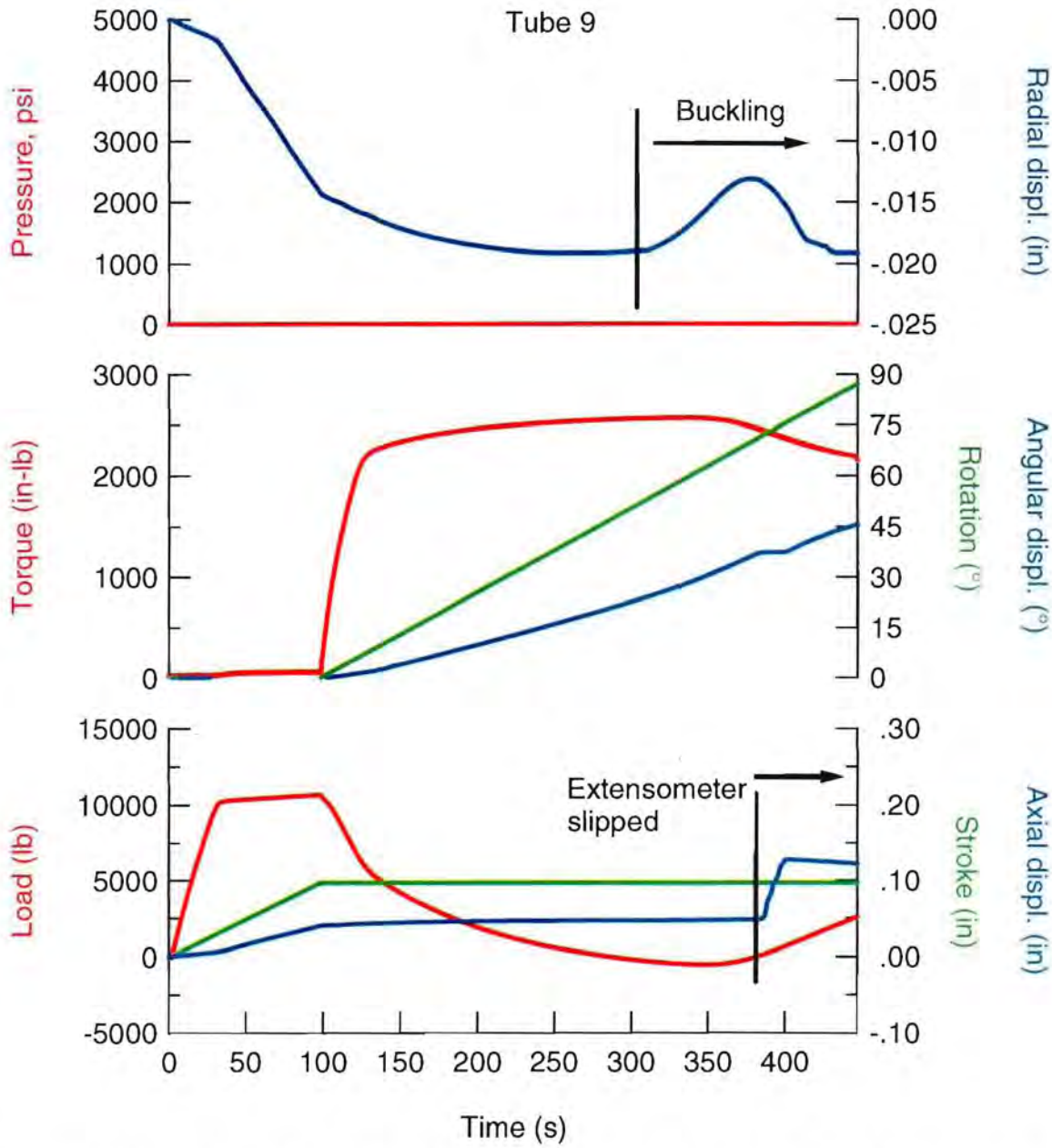

Figure 27. Load path 6 data (tube 9). Pressure was held at 0 psi. Stroke was ramped to the axial displacement gage reading of 0.04 in., followed by rotation to failure.

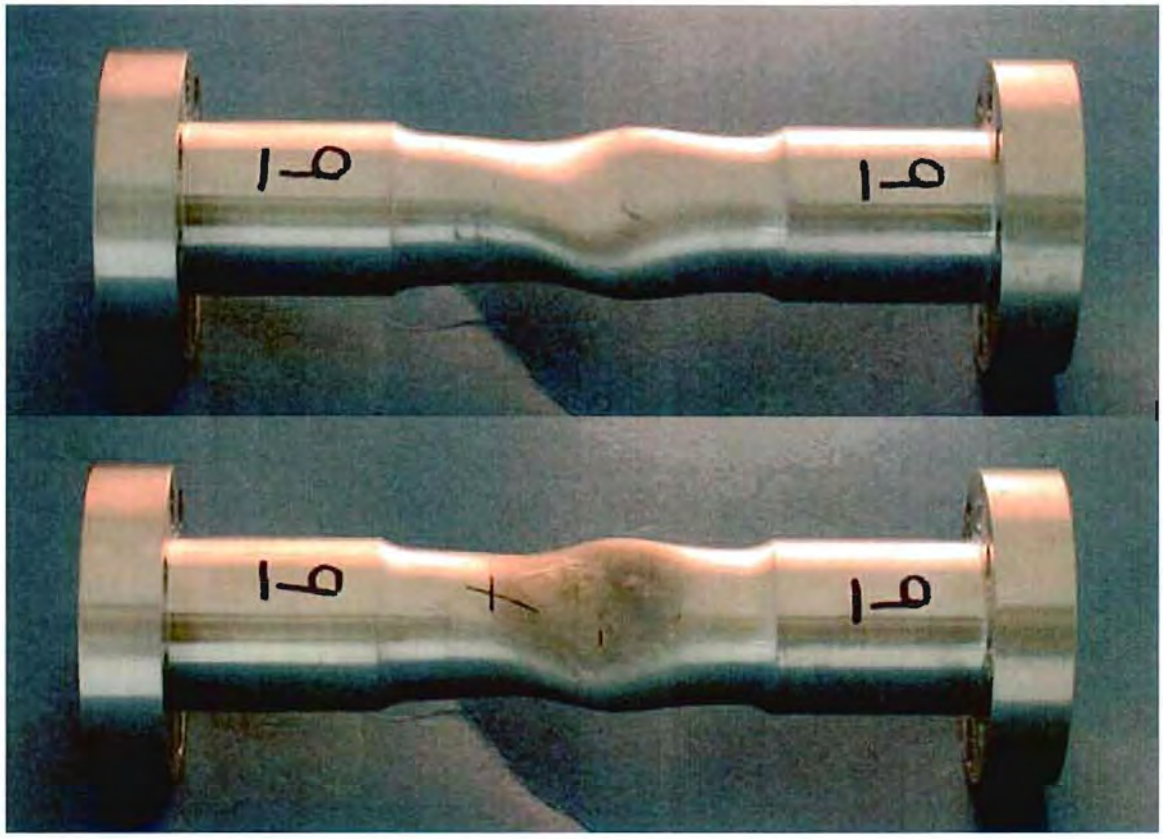

Figure 28. Post-test images of load path 6 specimen (tube 9). Torsional buckling is clearly visible.

3.2.4. Load paths 7 and 8: pressure, rotation, and stroke

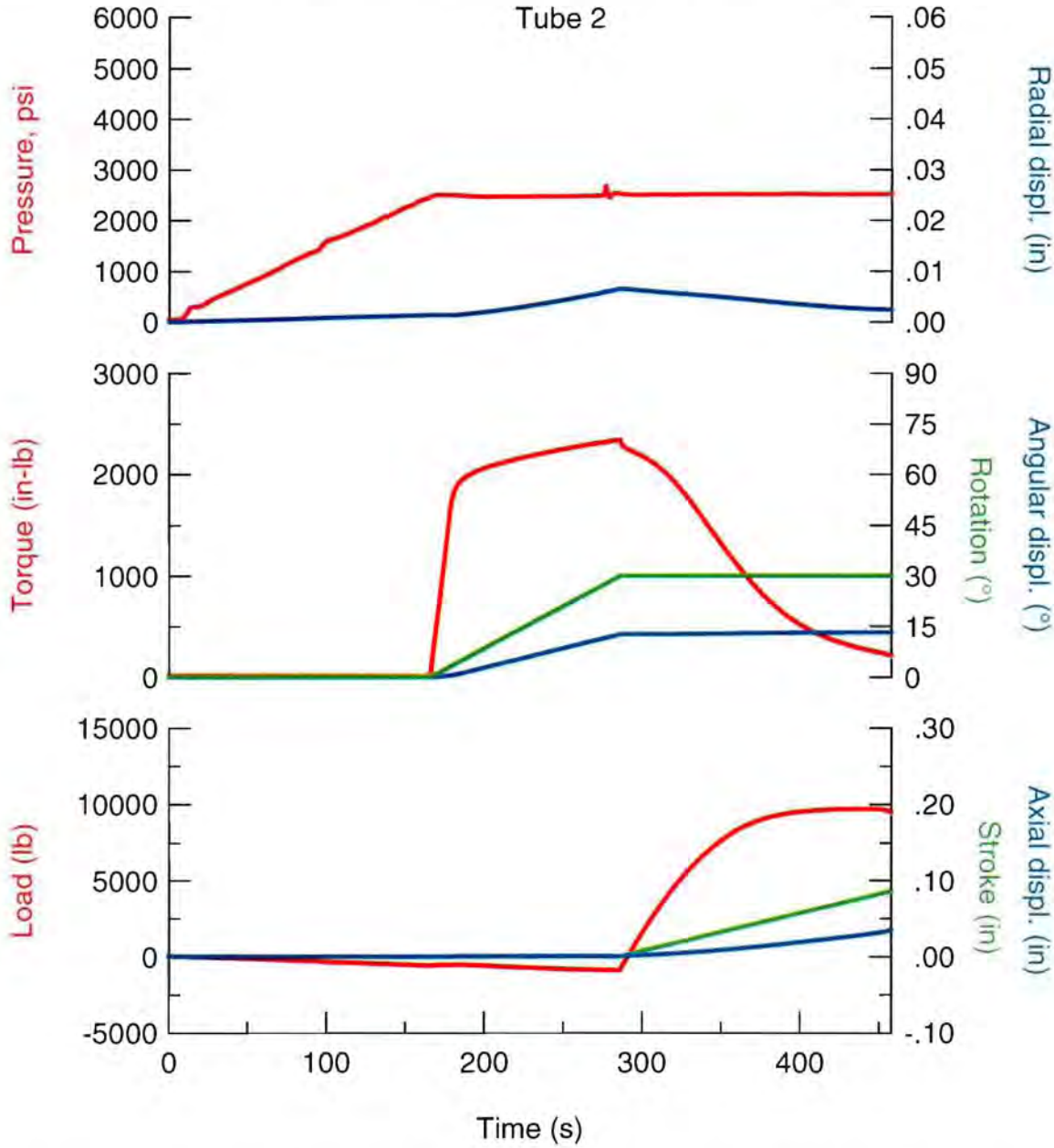

Figure 29. Load path 7 data (tube 2). Pressure was ramped to 2500 psi, followed by rotation to 30°. Stroke was then ramped to specimen failure.

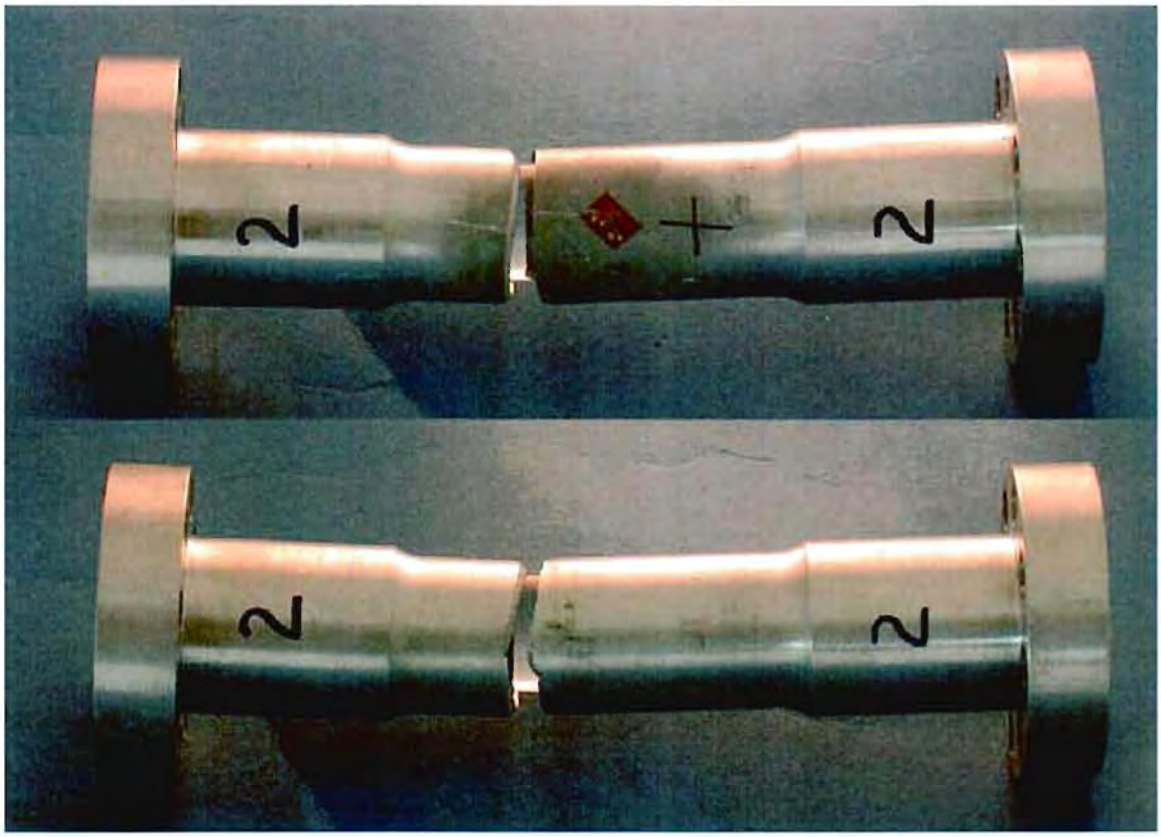

Figure 30. Post-test images of load path 7 specimen (tube 2).

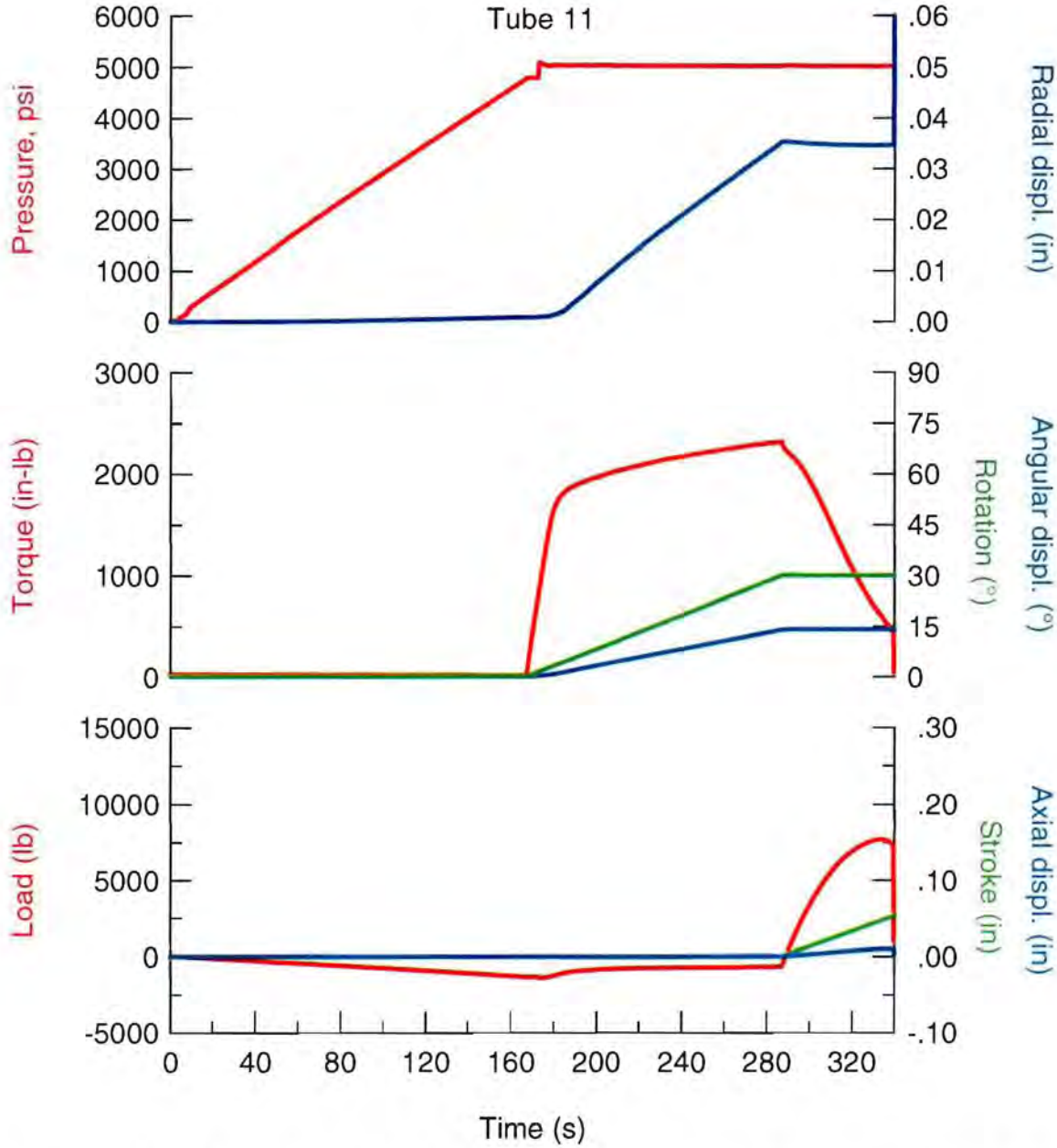

Figure 31. Load path 8 data (tube 11). Pressure was ramped to 5000 psi, followed by rotation to 30°. Stroke was then ramped to failure. The pressure showed a plateau followed by small jump to the target level of 5000 psi.

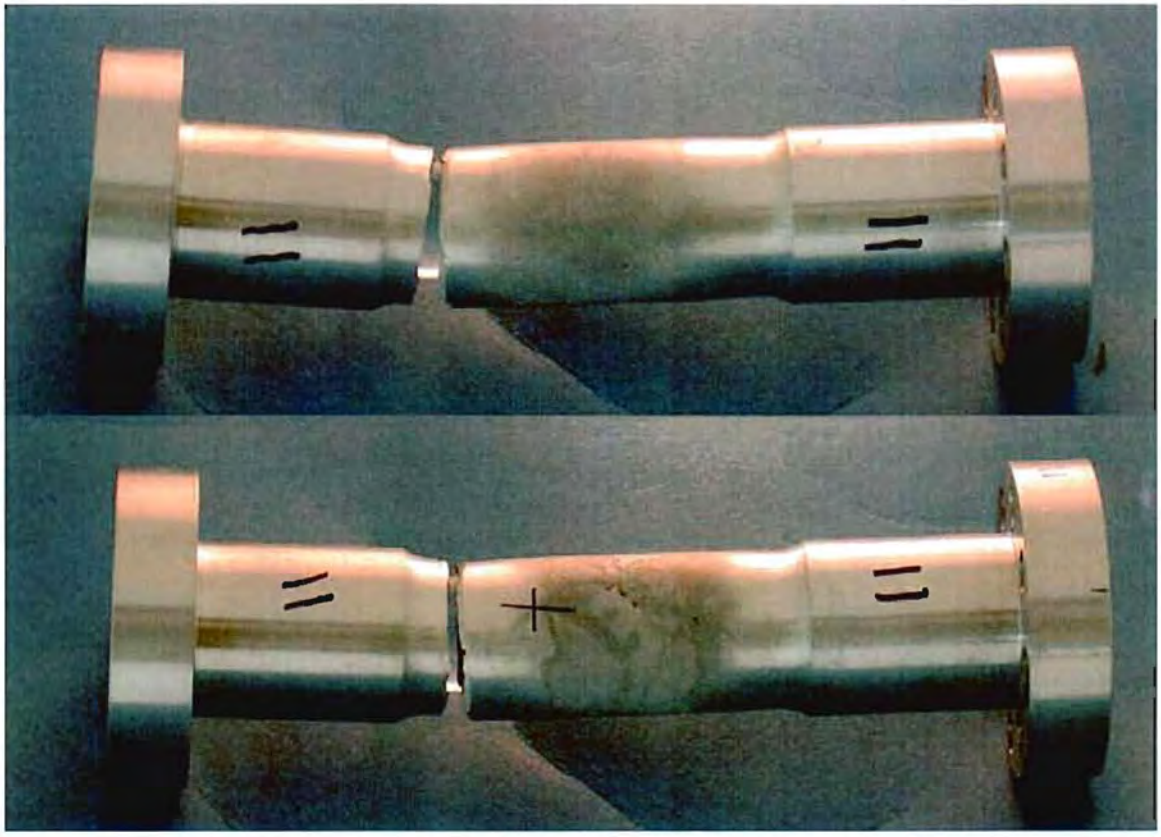

Figure 32. Post-test images of load path 8 specimen (tube 11).

3.2.5. Load path 9: pressure and rotation

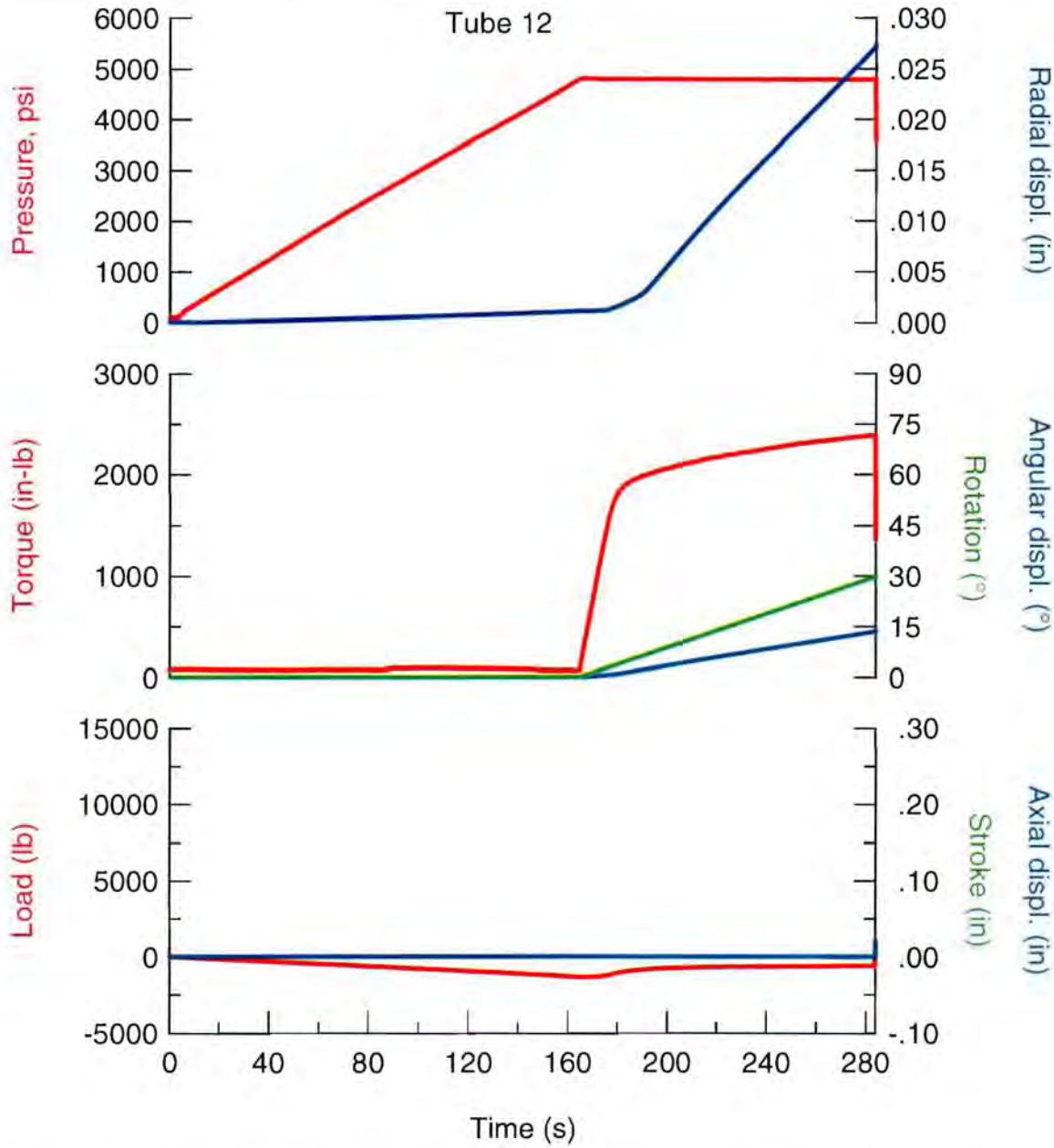

Figure 33. Load path 9 data (tube 12). Stroke was held at 0 in. Pressure was ramped to 5000 psi, followed by rotation to failure.

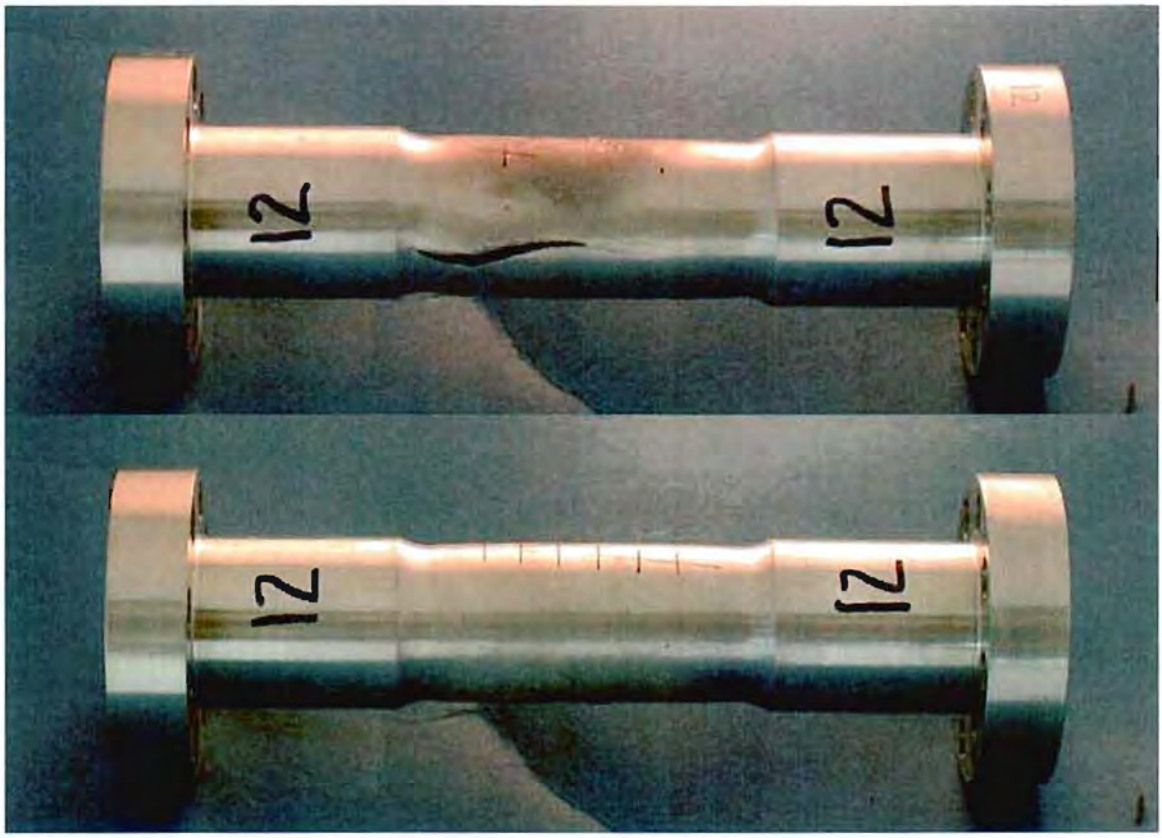

Figure 34. Post-test images of load path 9 specimen (tube 12). Although failure occurred during rotation, the orientation of fracture was strongly influenced by the internal pressure.

3.2.6. Load path 10: pressure and stroke

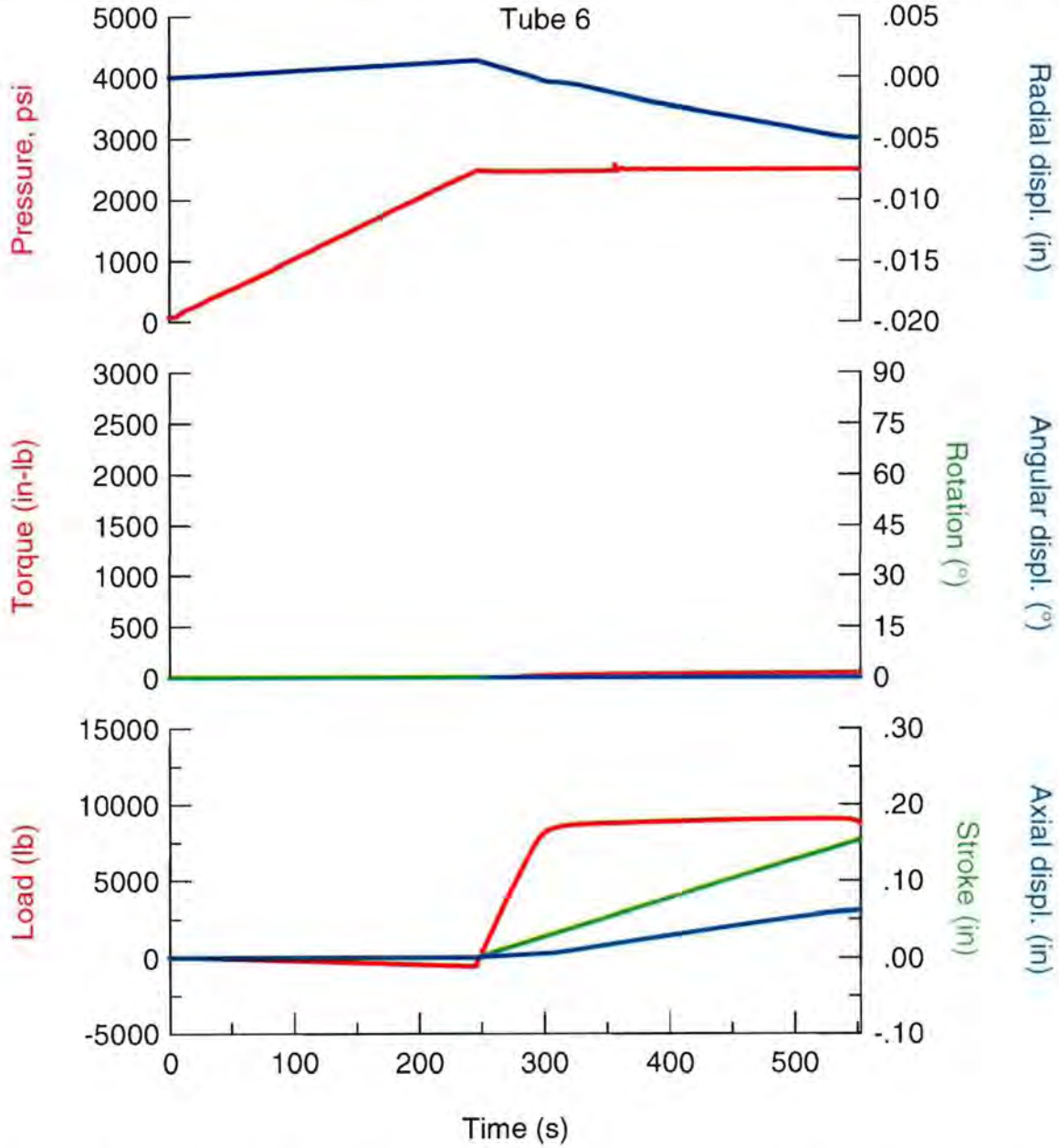

Figure 35. Load path 10 data (tube 6). Rotation was held at 0°. Pressure was ramped to 2500 psi, followed by stroke to failure.

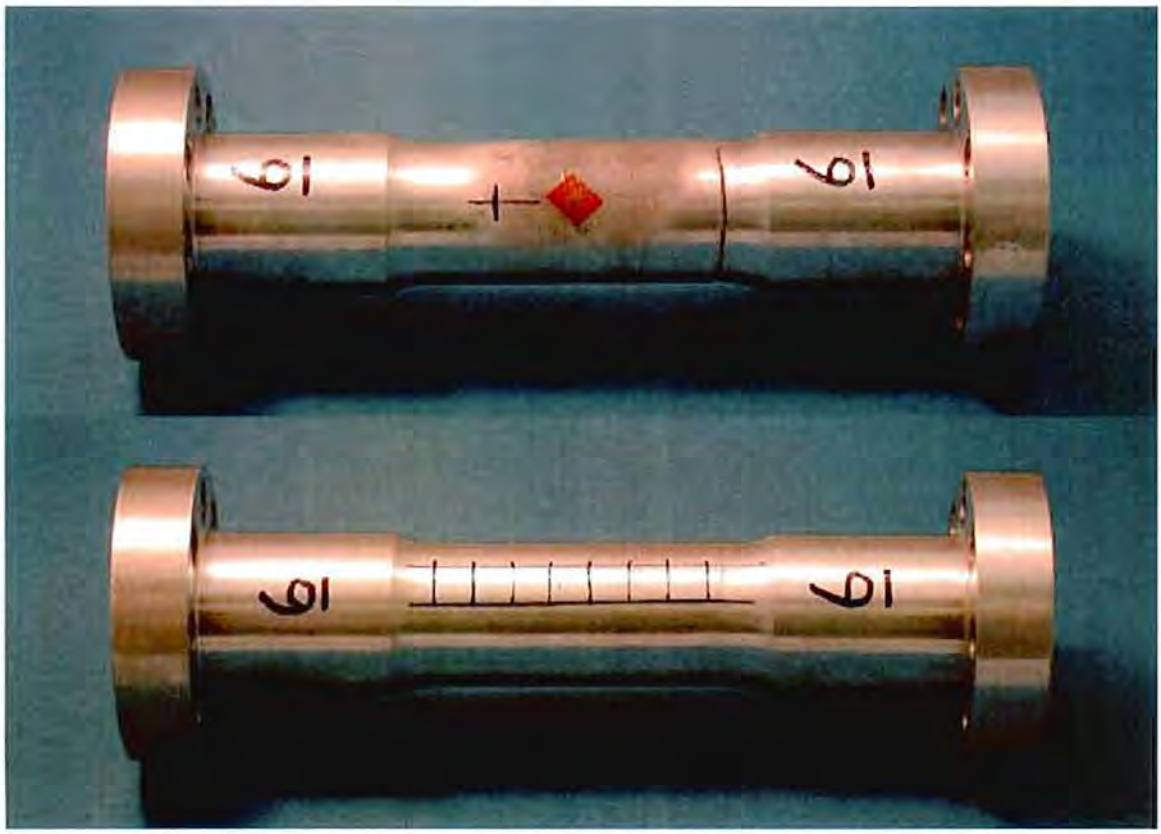

Figure 36. Post-test images of load path 10 specimen (tube 6).

3.2.7. Machine compliance

Machine compliance was measured for axial and torsional loading of the test frame using the solid steel specimen described in the section on experimental details. Figure 37 shows the axial compliance data and the calculated compliance correction curve, which is the displacement difference between the stroke measurement and the calculated elastic displacement of the solid steel link. A linear fit of the axial compliance correction curve had a slope of 6.92 in./lb. A second-order polynomial fit of the compliance correction curve with the form $y = K_0 + K_1(\text{load}) + K_2(\text{load})^2$ had the following coefficients: K_0 = 8.886e–5, K_1 = 4.972e–7, and K_2 = 1.053e–11.

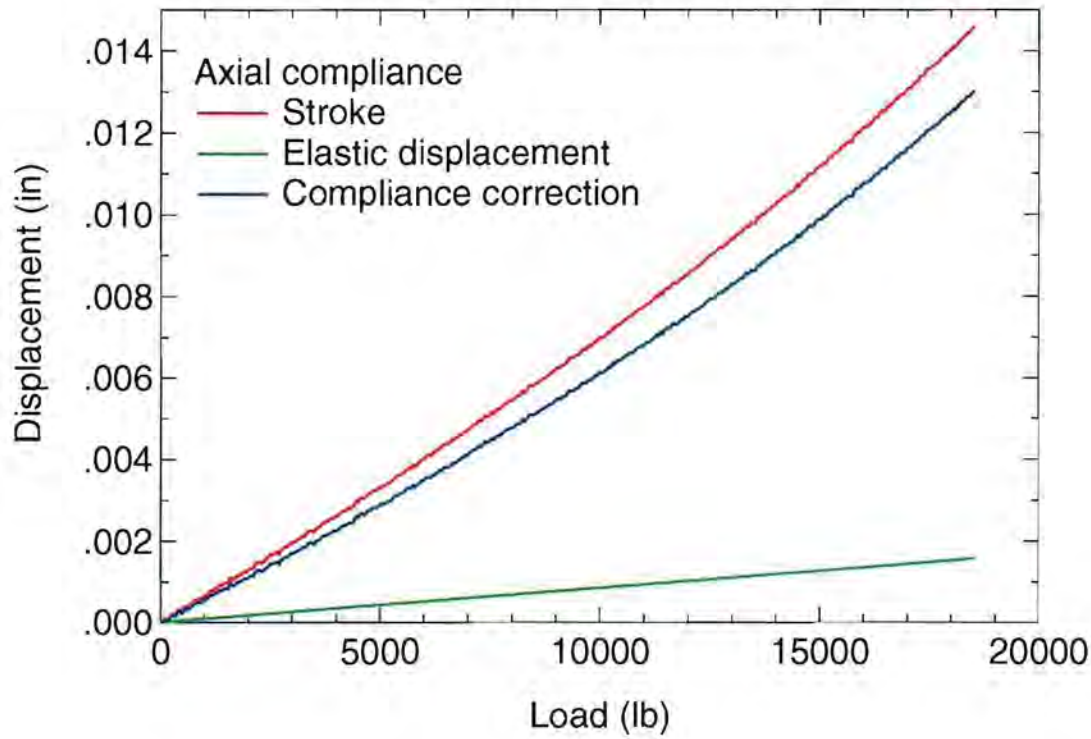

Figure 37. Axial compliance data. The compliance correction curve is the displacement difference between the stroke measurement and the calculated elastic displacement of the solid steel link.

Torsional compliance data is shown in Figure 38. A linear estimate of the compliance correction curve had a slope of 3.452e–5 degrees/in.-lb. A second-order polynomial fit of the compliance correction curve with the form $y = K_0 + K_1(\text{torque}) + K_2(\text{torque})^2$ had the following coefficients: $K_0 = 9.130e{-4}$, $K_1 = 2.967e{-5}$, and $K_2 = 8.021e{-10}$.

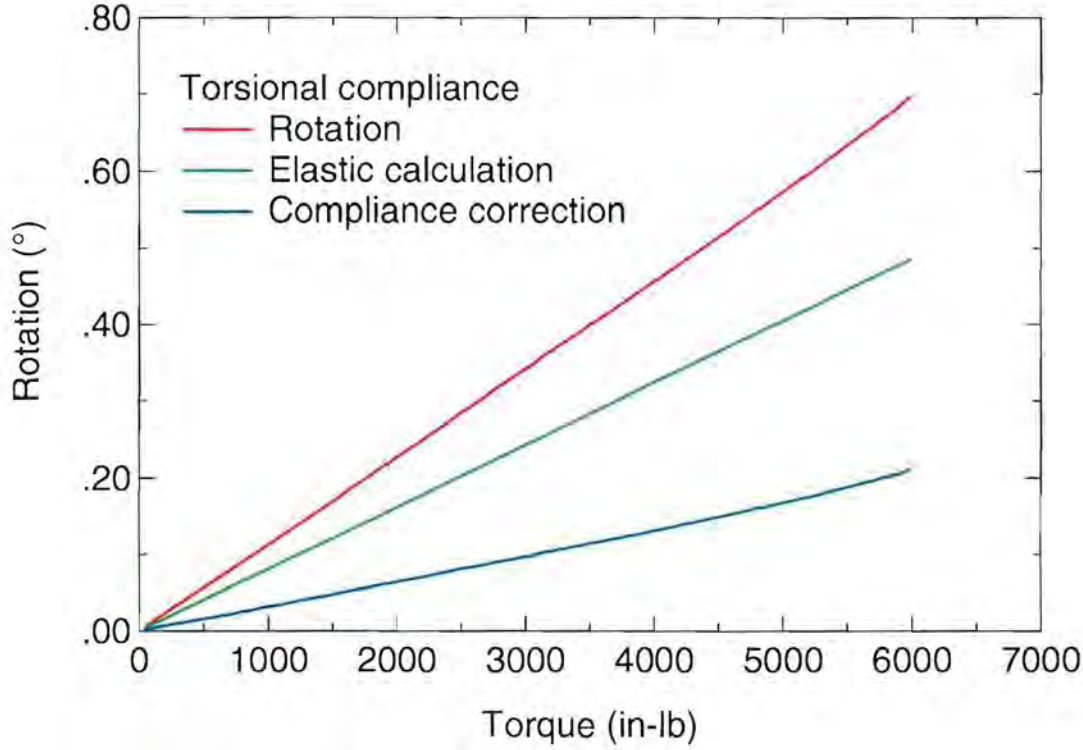

Figure 38. Torsional compliance data. The compliance correction curve is the angular displacement difference between the rotation measurement and the calculated elastic displacement of the solid steel link.

This page intentionally left blank.

4. COMMENTS

The tensile properties for the material used in this study are higher than commonly measured and higher than typical handbook values for 6061-T651. Good laboratory practice, agreement between data measured in New Mexico and California, and agreement between our data and the tensile properties listed on the material certification shown in Appendix A, provide confidence in using the data presented here for model validation. However, model parameters obtained from this data may not be appropriate for other lots or product forms of 6061-T6.

The validation experiments did not reveal surprising results. The interactions between loading paths can be understood through established concepts of mechanical behavior. The value of this effort lies in providing experimental data for comparison to material model simulations of path-dependent plasticity and failure.

Generally, it is good practice to perform replicate experiments for any given set of conditions. In this case, replicates of individual validation experiment loading paths were not completed, primarily due to cost and time constraints. The level of scatter in the calibration data for 6061-T651 suggests that scatter can affect the results of combined loading experiments in cases where individual steps within different loading paths reach critical levels. For example, the results for loading paths 8 and 9 suggest that a step 1 pressure near 5000 psi can produce failure in step 2 rotation to 30°, or the specimen may not fail until step 3 stroke. However, there are many similar conditions between the different loading paths that can be used to increase the confidence that significant differences in behavior would not be revealed through replicate experiments.

In the event that additional combined loading experiments were to be performed, a few refinements to the setup should be made. The diametric displacement gages should be modified to cover the full range of specimen diameter change, although this was only an issue with load path 3. The pressure system should be evaluated in an effort to reach the maximum command level with better accuracy and to eliminate pressure jumps. These are control issues that might be resolved by tuning or pressure sensor selection. The range of the torsional actuator was sufficient for all of the experiments except loading path 5, where torque control during a stroke ramp was desired. If similar experiments were to be conducted in the future, the use of a different axial torsional load frame with a larger rage of rotation might be an option. A 50-kip frame is available in this department that has a 10-turn range, but control issues would have to be resolved prior to performing the experiments.

This page intentionally left blank.

5. REFERENCES

[1] Materials Weapon Information System and Data Management application, http://www-irn.sandia.gov/wisdm/

[2] Materials Weapon Information System and Data Management application, http://www-irn.sandia.gov/wisdm/, Catalog:\Metals\Aluminum Alloys\Aluminum 6061\T651, Test Suite: 6061-T651, 4 in diameter rod.

[3] ASTM Designation D: D 5379/D 5379M-05, Standard Test Method for Shear Properties of Composite Materials by the V-notched Beam Method, ASTM International (2005).

[4] N. Iosipescu, "New accurate procedure for single shear testing of metals," *J. Mater.*, 2(3), 537–566 (1967).

[5] H. –C. Wu, Z. Xu. "An axial-torsional extensometer for finite deformation," *J. Eng. Mater. Tech. Trans. ASME*, 112, 330–335 (1990).

This page intentionally left blank.

APPENDIX A: MATERIAL CERTIFICATION 6061-T651

ALCOA

ALCOA EXTRUSIONS, INC.
1550 KIRBY LANE
SPANISH FORK, UT
84660

Alcoa Extrusions, Inc. a subsidiary of Alcoa Inc

Certified Inspection Report

Cert Number	Page
AEP257039	1 of 2
Cert Creation Date	**Cert Print Date**
31-JAN-05	31-JAN-05

Sales Order Number	Customer P/O
1352833 Line No. 2	45007

Invoice To Customer

TCI ALUMINUM / NORTH
2353 DAVIS AVENUE
HAYWARD, CA - 94545

Ship To Customer

TCI ALUMINUM / NORTH
2353 DAVIS AVENUE
HAYWARD, CA - 94545

Quantity Shipped	Date Shipped
1063 LB	31-JAN-05
B/L	**Item No.**
326066	G03370729
Delivery ID	**Item No. Rev**
443131	--
Customer Part No	
4ER	

Item Description

Extruded Econ-o-Rod
4 DIA
SECT 500330
144 IN LN
6061 / T6511
FIN M-MILL
W/F 14.778 F 01 CS 4
Marking CONTINUOUS;
ASTMB221 REV 04
AMS-QQ-A-200/8 REV
ASMESB221 REV
UNS#A96061 REV
SAEJ454 REV

Legal Statement

We hereby certify that, unless otherwise indicated, the material covered by this report has been manufactured, inspected, and tested in accordance with, and has been found to meet, the applicable requirements described herein, including any specifications forming a part of the description and that samples representative of the material met the composition and had the mechanical properties shown on the face of this certification. Also, note that mercury is not a normal contaminant in aluminum alloys and neither it nor any of its compounds are used in the manufacture of our product. This certification is not to be reproduced in partial form without prior written approval of our Quality Assurance Dept.

Signature And Title

D. Mark Shelley 31-JAN-05
Mark Shelley
Quality Control Manager

Quantities per Lot / Packages

Package Number	Lot Number	Quantity	UOM	Weight	
				Gross	Net
G14-PKG025737	1396272-C	6	PCS	1069	1063

Composition Limits

Alloy	Si		Fe		Cu		Mn		Mg		Cr	
	Min	Max	Min	Max	Min	Max	Min	Max	Min	Max	Min	Max
6061	0.40	0.8	---	0.7	0.15	0.40	---	0.15	0.8	1.2	0.04	0.35

Alloy	Zn		Ti		Others Each		Others Total	
	Min	Max	Min	Max	Min	Max	Min	Max
6061	---	0.25	---	0.15	---	0.05	---	0.15

Certified Inspection Report

ALCOA

ALCOA EXTRUSIONS, INC.
1550 KIRBY LANE
--
SPANISH FORK, UT
84660

Sales Order Number	Customer P/O
1352833 Line No. 2	45007

Cert Number	Page
AEP257039	2 of 2
Cert Creation Date	**Cert Print Date**
31-JAN-05	31-JAN-05

Mechanical Property - Test Limits

		Test Type	UTS - L		TYS- L		EL.4D-Long	
		UOM	KSI		KSI		PCT	
		# of Tests	-		-		-	
Test Temper	Lot Number	# of Tests	Min	Max	Min	Max	Min	Max
T6511	1396272	2	54.5	59.2	52.1	56.3	13.0	13.0

Cert Notes

Made in USA

APPENDIX B: SMOOTH TENSION SPECIMEN GAGE PROFILES

Smooth tension specimen gage profile measurements Raw stock location 1.356 in. diameter circle											
ID	Gage diameter (in)										
1	.2516	.2510	.2508	.2504	.2502	.2496	.2502	.2508	.2514	.2518	.2526
2	.2526	.2520	.2514	.2508	.2504	.2498	.2502	.2506	.2510	.2512	.2514
3	.2514	.2510	.2508	.2506	.2502	.2496	.2502	.2508	.2514	.2520	.2524
4	.2514	.2508	.2506	.2504	.2500	.2494	.2502	.2506	.2512	.2518	.2524
5	.2516	.2510	.2506	.2506	.2500	.2494	.2500	.2506	.2514	.2518	.2524
6	.2524	.2520	.2514	.2508	.2502	.2498	.2502	.2506	.2508	.2508	.2510
7	.2526	.2520	.2514	.2508	.2502	.2496	.2502	.2504	.2508	.2510	.2512
8	.2512	.2508	.2506	.2504	.2502	.2496	.2502	.2508	.2512	.2518	.2524
9	.2526	.2518	.2514	.2510	.2504	.2498	.2502	.2506	.2510	.2512	.2514
10	.2514	.2510	.2508	.2504	.2502	.2496	.2502	.2510	.2514	.2520	.2526
11	.2514	.2510	.2508	.2506	.2502	.2496	.2502	.2508	.2512	.2520	.2524
12	.2524	.2518	.2514	.2506	.2502	.2496	.2502	.2504	.2508	.2510	.2514
13	.2516	.2512	.2508	.2506	.2502	.2498	.2504	.2508	.2516	.2520	.2526
14	.2516	.2510	.2508	.2504	.2500	.2494	.2502	.2506	.2512	.2520	.2524
15	.2526	.2518	.2514	.2508	.2502	.2496	.2502	.2504	.2508	.2510	.2514

Smooth tension specimen gage profile measurements Raw stock location 2.646 in. diameter circle											
ID	Gage diameter (in)										
16	.2526	.2522	.2514	.2508	.2502	.2496	.2502	.2506	.2508	.2510	.2514
17	.2526	.2520	.2514	.2508	.2504	.2496	.2502	.2506	.2508	.2510	.2514
18	.2514	.2512	.2506	.2502	.2500	.2494	.2500	.2506	.2512	.2518	.2524
19	.2526	.2522	.2516	.2510	.2504	.2498	.2504	.2506	.2510	.2510	.2514
20	.2516	.2512	.2508	.2506	.2502	.2496	.2504	.2508	.2512	.2520	.2526
21	.2524	.2520	.2514	.2508	.2502	.2496	.2502	.2506	.2508	.2510	.2514
22	.2514	.2510	.2508	.2506	.2502	.2498	.2504	.2512	.2516	.2520	.2528
23	.2524	.2520	.2512	.2506	.2502	.2496	.2500	.2504	.2508	.2510	.2514
24	.2526	.2520	.2514	.2508	.2506	.2498	.2502	.2508	.2508	.2512	.2514
25	.2514	.2510	.2508	.2504	.2500	.2496	.2502	.2508	.2512	.2520	.2526
26	.2514	.2512	.2508	.2506	.2504	.2498	.2504	.2508	.2514	.2520	.2526
27	.2524	.2520	.2514	.2506	.2502	.2496	.2502	.2504	.2508	.2510	.2514
28	.2526	.2520	.2514	.2508	.2502	.2496	.2502	.2504	.2508	.2510	.2514
29	.2524	.2520	.2514	.2508	.2502	.2496	.2500	.2504	.2508	.2510	.2514
30	.2514	.2512	.2508	.2506	.2502	.2498	.2502	.2510	.2514	.2520	.2524

Smooth tension specimen gage profile measurements Transverse specimens											
ID	Gage diameter (in)										
T1	.2516	.2512	.2509	.2506	.2501	.2498	.2502	.2505	.2507	.2511	.2514
T2	.2517	.2514	.2510	.2507	.2503	.2499	.2504	.2507	.2510	.2513	.2516
T3	.2519	.2516	.2512	.2509	.2505	.2500	.2505	.2507	.2509	.2513	.2516
T4	.2516	.2514	.2510	.2506	.2502	.2498	.2503	.2506	.2508	.2512	.2514
T5	.2515	.2512	.2507	.2505	.2502	.2496	.2500	.2503	.2505	.2509	.2512
T6	.2514	.2511	.2508	.2507	.2503	.2497	.2500	.2505	.2509	.2511	.2514

DISTRIBUTION

1	MS0372	J. T. Ostien	1524
1	MS0372	J. Pott	1524
1	MS0372	W. M. Scherzinger	1524
1	MS0372	G. W. Wellman	1525
1	MS0555	P. W. Hatch	1522
1	MS0557	B. R. Rogillio	1521
1	MS0824	T. Y. Chu	1500
1	MS9042	B. R. Antoun	8776
1	MS9042	D. J. Bammann	8776
1	MS9042	E. P. Chen	8776
1	MS9042	M. L. Chiesa	8774
1	MS9042	J. J. Dike	8774
1	MS9409	J. S. Korellis	8776
1	MS9409	S. X. McFadden	8776
1	MS9161	K. L. Lee	8758
2	MS9018	Central Technical Files	8945-1
1	MS0899	Technical Library	9536

273934

Technical Library, 9616
MS 0899 (1)

Sandia National Laboratories